의학박사 학위논문

Hyperglycemia-induced Jagged 1 overexpression in endothelial cells causes retinal capillary regression in a murine model of diabetes mellitus

혈관내피세포에서 고농도 당에 의한 Jagged1 발현 증가와 당뇨병성 혈관병증의 병인기전에 관한 연구

2016 년 08 월

서울대학교 대학원
의과학과 의과학전공
최 영 은

A thesis of the Degree of Doctor of Philosophy

혈관내피세포에서 고농도 당에 의한 Jagged1 발현 증가와 당뇨병성 혈관병증의 병인기전에 관한 연구

Hyperglycemia-induced Jagged 1 overexpression in endothelial cells causes retinal capillary regression in a murine model of diabetes mellitus

August 2016

The Department of Biomedical Sciences
Seoul National University
College of Medicine
Young Eun Choi

ABSTRACT

Introduction: Regulation of vascular morphogenesis (sprouting, branching, lumenization, regression) by Notch signaling has been well characterized during vascular development. In adult mature vasculature, resting endothelial cells (ECs) also retain their growth potential that is activated under certain circumstances, but less is known about the maintenance mechanism of endothelial homeostasis.

Methods: We developed an *in vitro* model of human angiogenesis. Human ECs and smooth muscle cells (SMCs) in spheroid were co-cultivated on SMC monolayer under high glucose or control conditions.

For *in vivo* loss-of-function studies, we used both EC-specific *Jagged1* (*Jag1*) heterozygous deficient mice (*Tie2-Cre+;Jag1*$^{flox/+}$) and ECs-specific inducible *Jag1* deficient mice (*Tie2-CreER*^{T2}*+; Jag1*$^{flox/flox}$).

Results: Using the *in vitro* angiogenesis model, we observed high glucose-induced abnormal angiogenesis characterized by increased sprouting and branching points, decreased vascular diameter and length, and destabilization of the tubes. As the

underlying mechanism, we identified the PKC- and NF-κB-dependent upregulation of *Jag1* in ECs under high glucose condition.

Increased expression of *Jag1* was also observed in retinal ECs of streptozotocin-induced diabetic model. We confirmed attenuation of hyperglycemia-induced retinal vascular abnormalities in EC-specific *Jag1* deletion mice.

Conclusions: We found that increased expression of *Jag1* might be a mechanism of diabetic microvasculopathy. Correction of the pathologic angiogenesis by modulating the aberrant signaling in the present study highlighted a future direction of treatment of diabetic vasculopathy other than glucose control.

*Some of these works are published in Journal of Molecular and Cellular Cardiology. 2014 Apr;69:52-66., Circulation. 2016 Jul 12. [Epub ahead of print].

Keywords: Diabetes mellitus, microvasculopathy, Notch signaling
Student number: 2008-31033

CONTENTS

LIST OF TABLES AND FIGURES

Chapter 1

Chapter 2

LIST OF ABBREVIATIONS

ECs, Endothelial cells

SMCs, Smooth muscle cells

Jag1, Jagged1

Dll4, Delta-like 4

DM, Diabetes mellitus

VEGF, Vascular endothelial growth factor

NICD, Notch intracellular domain

PBS, Phosphate-buffered saline

GFP, Green fluorescence protein

NF-κB, Nuclear factor-κB

PKC, Protein kinase C

ROS, Reactive oxygen species

TBHP, Tert-butyl hydroperoxide

PCR, Polymerase chain reaction

STZ, Streptozotocin

RM, Retinal microvasculopathy

OHT, 4-hydroxytamoxifen

DAPT, N-[(3,5-Difluorophenyl)acetyl]-L-alanyl-2-phenylglycine-1,1-dimethylethyl ester

GENERAL INTRODUCTION

Microvessels consist of arterioles, capillaries, and venules. Among them, capillaries have the largest area and regulate permeability and myogenic responses that can adapt flow to local metabolic needs in contrast to larger vessels supplying blood to organs. Disturbances in capillaries are hard to be measured clinically. It may arise before overt hyperglycemic vascular pathologic changes. This diagnostic difficulty obscures the importance of the distinct role of the capillaries in the natural history of diabetes mellitus (DM). Aberration in the hyperglycemic microvasculature can reduce organ perfusion, particularly affecting organs dependent on their microvascular flow, namely the retina, kidneys, myocardium and peripheral nervous system. The clinical diseases associated with these changes—retinopathy, nephropathy, cardiomyopathy and neuropathy— cause a large burden of diabetic morbidity. Microvasculopathy also contributes to peripheral vascular disease and poor wound healing. To some extent, diabetic microvascular disease has been overlooked in terms of its clinical impact and research attention, in part, because there is

neither an established clinical tool for diagnosis nor an effective therapeutic option. Therefore, further investigation of microvascular disease should begin with regard to a novel therapeutic target of the microvasculature.

CHAPTER 1

High glucose-induced Jagged1 in endothelial cells disturbs Notch signaling for angiogenesis: A novel mechanism of diabetic vasculopathy

INTRODUCTION

Angiogenesis, the growth of new blood vessels from pre-existing vasculature, is a multistep process that involves sprouting, branching, lumenized tube formation and stabilization with recruiting pericytes or SMCs[1]. Recent studies provided tremendous insights into fundamental aspects of angiogenesis that have led to a mechanistic model of vessel sprouting and branching including Notch pathway in physiologic or pathologic angiogenesis[1-3]. The formation, extension and anastomosis of endothelial sprouts at the leading edge of the growing vessel front of neonatal murine retina lead to the generation of an immature network, which is strongly controlled by Notch and vascular endothelial growth factor (VEGF) signaling[4]. Notch receptors and the ligands delta-like 4 (Dll4) and Jag1 regulate the dynamic and transient selection of filopodia-extending endothelial cells (tip cells), which lead and guide vascular sprouts. Once the Notch extracellular domain interacts with a ligand, γ-secretase cleaves the Notch intracellular domain (NICD) of the Notch protein. This releases the NICD, which then moves to the nucleus, where it can regulate gene

expression by activating the transcription factors. Dll4 expression in tip cells leads to the activation of Notch in adjacent ECs, and induces a stalk-like phenotype characteristic of cells at the base of sprouts[5]. The vessel-stabilizing activity of Dll4-Notch is opposed by Jag1, which has pro-angiogenic activity and is highly expressed by stalk cells and in the immature vessel plexus[6]. Therefore, the balance between Dll4 and Jag1 seems to control vascular growth via Notch signaling modulation.

Most of the data from previous studies have been acquired in a murine neonatal retina angiogenesis model[4-6]. Human angiogenesis has not been thoroughly elucidated due to a lack of a proper model for studying intercellular signaling. Several *in vitro* models bridges *in vitro* and *in vivo* angiogenesis such as embryoid body-derived vascular system[7], the aortic ring culture[8], and most recently a mixture of endothelial and mesenchymal cells for three-dimensional vascularization of liver tissues created *in vitro*[9]. However, there still remains much to be improved.

On the other hand, the major problem in patients with DM is vascular complication which consists of macrovasculopathy and

microvasculopathy [10-12]. Several mechanisms are suggested for vasculopathy or pathologic angiogenesis[13-16]. However, diabetic vasculopathy has not been studied in terms of intercellular signaling between tip, stalk and phalanx cells, which controls angiogenesis and vascular stabilization.

To gain a proper model of multistep human angiogenesis in a high glucose condition, we developed a novel *in vitro* 2-dimensional angiogenesis model like the murine retinal angiogenesis using co-cultivation of human ECs and human vascular SMCs in a spheroid on an SMC monolayer. This model enabled us to characterize the effect of high glucose condition on human angiogenesis which was mediated by an abnormal Notch signaling in the present study.

MATERIALS AND METHODS

1. Isolation of human ECs and human SMCs

ECs and SMCs were isolated from mesenteric and gastroepiploic arteries as described earlier[17] with some modifications. The institutional review board of Seoul National University Hospital approved the protocol of isolation of ECs and SMCs from the arteries of the resected stomach due to cancer (IRB number: H-0910-006-295). In brief, the vessel surface was rinsed off and the fat or connective tissue was removed in cold phosphate-buffered saline (PBS), and then a 25-gauge catheter was inserted. The inside of the lumen was washed with a cold PBS and filled with 0.1% type II collagenase (Gibco, Carlsbad, CA, USA) in PBS. After incubation for 10 minutes at 37℃, ECs were collected by flushing with 2 ㎖ of EGM-2MV (Lonza, Verviers, Belgium) and plated on 1.5% gelatin (Sigma Aldrich, St. Louis, MO, USA)-coated dishes. Incubation with the collagenase solution and flushing with the media were repeated 5 times. After the removal of ECs, the remaining tissue was cut into pieces and digested with 0.5% collagenase in PBS. After incubation for 4 hours at 37℃ in a

shaking incubator, the digest was filtered through a 70-μm cell strainer (BD Pharmingen, San Diego, CA, USA) and cells were collected by centrifugation. It was then suspended in low glucose DMEM (Gibco, Carlsbad, CA, USA) containing 10% FBS and plated on 0.1% gelatin-coated dishes. Bone marrow mononuclear cells from healthy volunteers were isolated from bone marrow aspirates by density gradient centrifugation as previously described[18].

2. Lentiviral transduction

To visualize cell behavior in real time, we used a lentivirus-based transduction system as described previously[19]. We used lentiviral vectors that contained the enhanced green fluorescence protein (GFP), yellow fluorescence protein (YFP, Clontech, Palo Alto, California, USA), and cyan fluorescence protein (CFP, Clontech, Palo Alto, California, USA). To further investigate the effect of gene overexpression, we subcloned a construct encoding *Jag1* cDNA (Open Biosystems, Huntsville, AL, USA) into the lentiviral vector.

We utilized the lentiviral vector pLentiLox 3.7 (pLL3.7)[20] expressing shRNA to knockdown the expression of endogenous

Jag1 targeting the sequence 5′ -GTGCACCTCTGACTCC-3′ . A scrambled sequence, 5′ -CAACAAGATGAAGAGCACCAA-3′ , was used as a control. We co-transfected lentiviral constructs with packaging vectors into 293T cells by polyethylenimine (Polyscience, Warrington, PA, USA) and collected the supernatants containing lentiviral particles after 48 hours. We transfected the target cells twice by adding the viral supernatants to the cell-specific medium. Transduction efficiency was over 98% for ECs.

3. Generation of an angiogenesis model using ECs and SMCs: a hybrid spheroid

In order to make the best vessel-like structures from the spheroid, we tried several different conditions in terms of total cell number per spheroid (ranging from 1×10^3 to 1×10^4) and ratio of ECs/SMCs (1:1, 2:1, 1:2). Then, we fixed the number of cells to three thousand ECs/spheroid with a 2:1 ECs:SMCs ratio for our experiments.

For the preparation of the hybrid spheroids, we suspended a mixture of GFP-transduced ECs and non-labeled SMCs in

EGM (Lonza, Verviers, Belgium) containing 20% MethoCult (StemCell Technologies, Vancouver, Canada) and then cultured them in conical-bottom 96-well plates (Nunc, Wiesbaden, Germany). After 24 hours, we harvested the spheroids and then seeded them in collagen gels (Chemicon, Tenecula, CA, USA) or on an SMC monolayer in a dish with a cover glass bottom (μ-Dish, ibidi, Verona, WI, USA). We maintained culture for 7 days with medium change every other day.

4. Immunofluorescent staining and confocal microscopic analysis

Immunostaining was performed as described previously[21] with slight modifications. Briefly, cells were fixed with 4% paraformaldehyde for 30 minutes, permeabilized with 0.25% Triton X-100 in PBS for 5 minutes, and blocked with 1% bovine serum albumin in PBS for 1 hour. After blocking, cells were incubated overnight at 4℃ with specific primary antibodies: anti-Notch1 (Cell Signaling Technology, Danvers, MA, USA), anti-Jag1 (Santa Cruz Biotechnology, Santa Cruz, CA, USA), and anti-VE cadherin (Santa Cruz Biotechnology,

Santa Cruz, CA, USA) and followed by incubation with fluorescent tagged secondary antibodies (Invitrogen, Carlsbad, CA, USA). The images were acquired by a confocal laser scanning microscope system (LSM 710, Carl Zeiss AG, Oberkochen, Germany) and processed with Zen 2008 software (Carl Zeiss AG, Oberkochen, Germany). A water- or oil-immersion objective (40×, or 63×, 1.4 numerical aperture, NA) with the pinhole set for a section thickness of 0.8 ㎛ (pinhole set to 1 airy unit in each channel) was used. To visualize a 3D reconstructed image, a Z-stack of 20 ㎛ thickness was obtained. Diode (405 nm), Multi-Argon (488 nm), HeNe (543 nm), and HeNe (633 nm) laser lines were selected and images were acquired sequentially using separate laser excitations to avoid cross-talks between different fluorophores.

5. Analysis of reactive oxygen species

After 14 days of culture, the culture medium was changed to EGM. We added 1 mM N-acetylcysteine to the negative control sample and incubated it for 1 hour. And then we added 400 ㎛ tert-butyl hydroperoxide (TBHP) to the negative and positive control samples and incubated them for 1 hour. Then, we

incubated the samples for 1 hour with the 1mM CellROXDeep Red reagent (Life Technologies, Carlsbad, CA, USA). We acquired fluorescent images by confocal microscopy and then quantified the intensity of fluorescence in ECs.

6. Reverse transcription-polymerase chain reaction (RT-PCR)

We isolated total RNA using RNeasy RNA isolation kit (Qiagen, Valencia, CA, USA). We performed reverse transcription using 1 μg RNA with amfiRivert cDNA synthesis premix (GenDepot, Barker, TX, USA). We performed PCR using the following primers: for *Jag1*, 5′-CTCCTGTCGGGATTTGGTTA-3′ forward and 5′-CCACAGACGTTGGAGGAAAT-3′ reverse primers; for *Dll4*, 5′-ACCTTTGGGTGTCTGTCTGG-3′ forward and 5′-ACTTTTGGAAACACGGATGC-3′ reverse primers; for *GAPDH*, 5′-CGTGGAAGGACTCATGAC-3′ forward and 5′-CAAATTCGTTGTCATACCAG-3′ reverse primers. We measured PCR band intensity for quantification using Image J software (NIH, MD, USA).

7. Assessment of the activity of PKC isoforms in ECs under high glucose condition

ECs were seeded on a 1.5% gelatin-coated dish in EGM medium. ECs were incubated at 25.6mM of glucose or mannitol for 72 hours. We loaded 25 ㎍ of protein from the cell extract for western blot. We incubated the membrane with primary antibodies included in PKC and phospho-PKC isoform antibody sampler kit (Cell Signaling Technology, Danvers, MA, USA) at 1:1500 at 4℃ overnight.

8. Quantification and statistical analysis

We obtained images for comparative analysis under identical conditions of light, contrast and magnification. The sprouting area of the hybrid spheroid model was automatically measured by Image J software (NIH, MD, USA). To calculate sprout length, we drew lines on the image along the sprout and then measured the length of the lines using the software. We counted every point of branching from the spheroid for the number of branching points. All results are expressed as mean ± standard deviation. The differences of continuous variables

between experimental groups were analyzed by Student's t-test or one-way ANOVA using GraphPad Prism 5 (GraphPad Software, San Diego, CA, USA). To analyze the effect of time and treatments, we performed two-way ANOVA.

RESULTS

Multi-step process of the human angiogenesis in a spheroid model

The multistep process of angiogenesis in human cells could not be well presented by current *in vitro* angiogenesis models, for example, Matrigel tube formation assay or endothelial spheroid culture[22]. *In vitro* three dimensional collagen matrix models successfully demonstrated endothelial lumen formation, but such a three-dimensional matrix made it difficult for us to perform further immunofluorescent staining, confocal microscopic imaging and quantification[23, 24]. Therefore, we co-cultured GFP-transduced ECs with non-labeled SMCs in a spheroid on an SMC monolayer. We could observe, without further staining, the multistep process of angiogenesis which recapitulated the 2-dimensional developmental angiogenesis in the neonatal murine retina (Figure 1-1). First, ECs sprouted out of the spheroid (Figure 1-1a,b) leading to endothelial tube formation (Figure 1-1c). Tip cells, ECs with many filopodia (Figure 1-1d), stood at the front end of sprouts, led sprouting, and were followed by stalk cells (Figure 1-1e). Angiogenesis

in vitro was augmented by exogenous VEGF treatment as compared to the nontreated one (Figure 1-1c,f). As it maturated, multiple vacuoles developed and then capillary-like lumen appeared between adjacent ECs which were connected to each other by VE-cadherin (Fiture 1-1g,h,i). There was dynamic remodeling which included regressing, growing and newly appearing sprouts (Figure 1-1j,k). Stabilized tubes were supported by basement membrane which consisted of type IV collagen (Figure 1-1l,m). The remodeling process made connections among the sprouts and then formed a network of capillaries (Figure 1-1n).

High glucose concentration disturbed both sprouting activity of ECs and stabilization of endothelial tubes

Next, we evaluated the effect of high glucose concentration on the multi-step process of the human angiogenesis *in vitro*. When we cultivated the spheroids at several different glucose concentrations (5.6, 15.6, 25.6, 35.6 mM), we found that any glucose concentration higher than normal decreased the mean length of sprouting tubes from the spheroids. Then we fixed the high glucose concentration at 25.6 mM for the next experiments.

High glucose concentration, compared with normal, produced more sprouting tubes and filopodia at the tip cells with more frequent branches and tubes with smaller diameter (Figure 1-2a,b,c). When we continuously monitored the remodeling process of the preformed tubes at the same field for 72 h, we found that endothelial tubes in 25.6 mM of mannitol continuously grew and formed new vessels (Figure 1-2d, arrows) whereas those in 25.6 mM of glucose became thinner, regressed, and then disconnected (Figure 1-2d, arrow heads). Image quantification revealed that endothelial tubes in high glucose condition produced more new filopodia than control whereas they regress more than control (Figure 1-2e). When we added exogenous VEGF in the medium, we noted that the high glucose group showed many filopodia from EC tubes through type IV collagen breakage in contrast to the mannitol group (Figure 1-2f). We assessed the proliferation activity of ECs and SMCs in this spheroid depending on glucose concentration (Figure 1-2g). First, the proliferation activity was significantly higher in SMCs than in ECs regardless of glucose concentration. Second, there was an intriguing reciprocal pattern of cell proliferation by high glucose between

ECs and SMCs. Proliferation of ECs was suppressed by high glucose condition compared with mannitol at days 3 and 10. Proliferation of ECs was very low at day 10, which made the statistical analysis impossible. In contrast, SMCs responded to high glucose and showed higher proliferation activity at day 10 than when exposed to mannitol ($p = 0.004$). The apoptosis of ECs and SMCs in this model was similar between high glucose and control mannitol conditions at day 10 (Figure 1-2h).

Notch signaling has been reported to be closely related to proper formation and maintenance of the vascular system in several human and mouse genetic studies[1, 5, 6]. This model mimicked murine neonatal retina angiogenesis and thus enabled us to analyze each step of angiogenesis in association with Notch signaling. Especially, high glucose condition induced abnormal sprouting angiogenesis with changes in tip and stalk cells. Therefore, we evaluated Notch signaling molecules in a high glucose condition in the next step.

High glucose increased selectively *Jag1* expression via NF-κB and PKC pathway in ECs

First, we would like to find which molecule is regulated in response to high glucose condition in ECs and dissect the underlying mechanism. In previous reports, cell-to-cell contact influences expression of Notch signaling molecules[25-27]. Thus, we examined the effect of high glucose on the expression of the two vasculature-specific Notch ligands, Dll4 and Jag1, which showed distinct spatial expression patterns and opposing functional roles regulating angiogenesis[6] as well as their receptors, Notch 1 and 2, in ECs under both sparse and confluent culture conditions. In one of the Notch ligands, *Dll4*, expression was higher in confluent culture condition than in the sparse condition, while little to no expression of another Notch ligand, *Jag1*, was detected in the confluent condition (Figure 1-3a). Interestingly, however, when ECs were cultured under high glucose (25.6 mM) condition for 3 days, only *Jag1* expression was significantly induced both in sparse and confluent conditions (Figure 1-3a), whereas *Dll4* was not induced by high glucose. The amount of mRNA expression of *Notch* 1 or 2 was not affected by high glucose condition. We found that high glucose conditions increased both mRNA (Figure 1-3b) and protein (Figure 1-3c) expression of Jag1.

When we analyzed the relative expression of *Jag1* using real-time PCR, high glucose condition increased *Jag1* expression in ECs both in a dose- (3- and 3.5-fold increase at 25.6 mM), and time-dependent manner (5-and 7-fold increase after 6 day-exposure) compared to mannitol control (Figure 1-3d,e). In terms of the upstream regulator of *Jag1* in this model, we investigated the role of nuclear factor-κB (NF-κB) and protein kinase C (PKC) because NF-κB has been shown as a downstream molecule of tumor necrosis factor (TNF) for induction of *Jag1* expression in ECs [28] and because PKC was reported to be a mediator of diabetic vasculopathy[15, 29]. Induction of *Jag1* was attenuated by a PKC-412 compound, a non-specific inhibitor of PKC (Figure 1-3f). PKC is known as one of the upstream activators of NK-κB. We found that induction of *Jag1* by high glucose (25.6 mM) was also mitigated by NF-κB inhibitor, BAY 11-7082 (Figure 1-3g). Reactive oxygen species (ROS) are known to be involved with endothelial dysfunction in diabetes especially in ECs. Therefore we evaluated whether ROS was involved in the abnormal angiogenesis in our *in vitro* model. Positive control, TBHP significantly increased ROS in ECs and NAC reduced ROS in

ECs (Figure 1-3hi). We found that the high glucose condition in this model did not significantly increased ROS compared to the mannitol control.

High glucose increased Jag1 expression and decreased Notch signaling in ECs

To confirm if the abnormal Notch signaling in high glucose condition occurred in the spheroid model, we performed immunofluorescent staining of vasculature-specific Notch ligands, stimulatory Dll4 and inhibitory Jag1. Expression of Dll4 was not different between mannitol and glucose groups showing peri-nuclear spotty staining in ECs (Figure 1-4a). In contrast, Jag1 especially at tip cells showed diffuse strong staining with frequent nuclear enhancement (Figure 1-4b, arrow head) in the high glucose group in contrast to the diffuse dim staining in the mannitol group (Figure 1-4b). Then, we performed immunofluorescent staining of full-length Notch1, which showed both non-cleaved Notch and cleaved NICD. It showed a different nuclear translocation of Notch1 in the leading tip cells; extra-nuclear localization (only membrane and cytosol localization) in the high glucose condition, which means Notch

signaling inhibition, whereas prominent nuclear localization in the control condition (Figure 1-4c). The different staining pattern of Jag1 and Notch1 in the sprouting ECs was quantified in Figure 1-4d and Figure 1-4e, respectively. These findings suggest that high glucose increases the inhibitory ligand Jag1 leading to suppression of Notch signaling in ECs. To confirm association of the suppressed Notch signaling and the overexpressed Jag1, we co-stained NICD and Jag1. ECs with diffuse dim Jag1 staining showed strong nuclear translocation of NICD (Figure 1-4f, arrow head) whereas ECs with diffuse strong Jag1 staining and nuclear enhanced showed weak nuclear translocation of NICD, which confirms inhibition of Notch signaling in ECs with high Jag1 expression (Figure 1-4f, arrow).

Effect of Jag1 overexpression or Notch inhibition on human angiogenesis

Next, we evaluated whether Jag1 overexpression or inhibiting Notch signaling by γ-secretase inhibitor resulted in similar changes in the spheroid model. We transduced ECs with lentiviruses expressing Jag1 to evaluate the effect of Jag1

overexpression on angiogenic sprouting. Overexpression of Jag1 showed higher number of sprouts, filopodia at the tip cells and branching points and lower mean diameter of sprouts than control, which were similar changes to the high glucose condition (Figure 1-5a,b,c). Immunofluorescent staining demonstrated a prominent nuclear translocalization of NICD in the sprouting ECs in control (Figure 1-5d). In contrast, NICD was detected only at the membrane and cytosol in the Jag1-overexpression group suggesting Notch signaling inhibition in this group.

Patterns of sprouting and tube formation were significantly affected also by another Notch inhibitor, γ-secretase inhibitor like DAPT (N-[N-(3,5-difluorophenacetyl)-L-alanyl]-S-phenylglycine t-butyl ester) (Figure 1-5e,f). DAPT in the medium significantly induced more sprouts, filopodia at the tip cells and branching points from a spheroid and made tubes narrower than control medium did (Figure 1-5g). When we continuously monitored the remodeling process of the preformed tubes at the same field for 72 h, we found that endothelial tubes in the DAPT-treated group became thinner and more arborized after the process of transient growth,

regression, and then disconnection of tubes like those in the high glucose condition (Figure 1-5h). Endothelial tubes in the DAPT-treated group are active in the remodeling process of angiogenesis; more new filopodia, transient growth, and active regression, compared with control (Figure 1-5i).

High glucose-induced aberrant vascular growth was normalized by down-regulation of *Jag1*

Then, we evaluated whether endothelial cell-specific suppression of *Jag1* expression using lentiviral shRNA transduction would restore high glucose-induced abnormal angiogenesis. Transduction of lentivirus expressing GFP-labeled shRNA (scrambled or *Jag1*) did not alter endothelial morphology and growth (Figure 1-6a). We confirmed that *Jag1* was effectively down-regulated by *Jag1* shRNA transduction in ECs in contrast to scrambled shRNA (Figure 1-6b). Down-regulation of *Jag1* remarkably restored aberrant angiogenesis; the decreased diameter, increased sprouts and branching points induced by exposure to high glucose (Figure 1-6c,d).

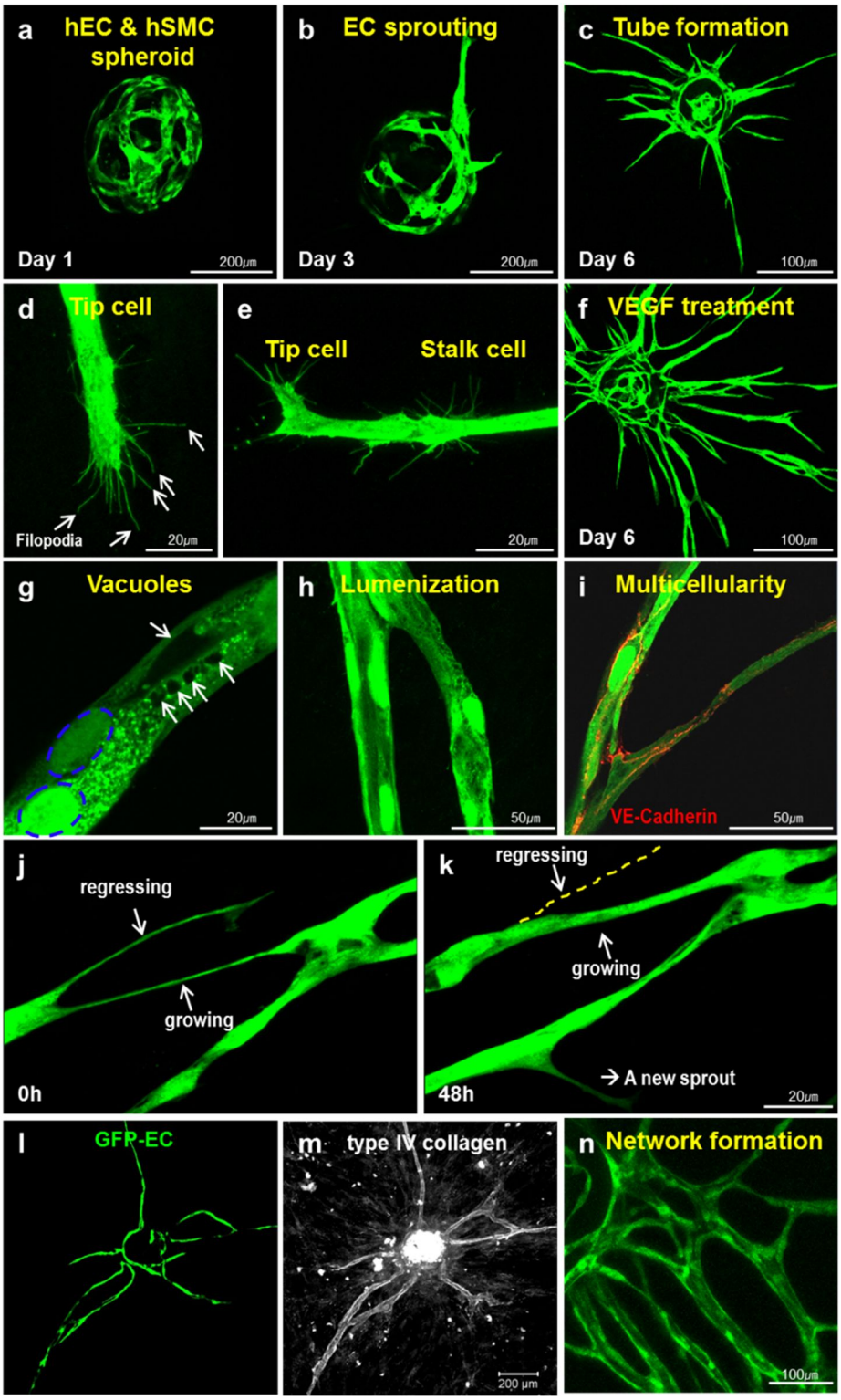
a hEC & hSMC spheroid
Day 1
200μm
b EC sprouting
Day 3
200μm
c Tube formation
Day 6
100μm
d Tip cell
Filopodia
20μm
e
Tip cell
Stalk cell
20μm
f VEGF treatment
Day 6
100μm
g Vacuoles
20μm
h Lumenization
50μm
i Multicellularity
VE-Cadherin
50μm
j
regressing
growing
0h
k
regressing
growing
→ A new sprout
48h
20μm
l GFP-EC
m type IV collagen
200 μm
n Network formation
100μm

Figure 1-1. *In vitro* model of multi-step sprouting angiogenesis. a) Co-cultured GFP-transduced EC with non-labeled SMC in a spheroid on SMC monolayer in a coverglass-bottom dish on day 1. b) Spouting from the spheroid on day 3. c) Multiple endothelial tubes from the spheroid on day 6. d) Vivid filopodia of a tip cell without additional staining. e) Tip cells followed by stalk cells. f) Augmented angiogenesis by exogenous 10ng/ml VEGF treatment as compared to non-treated one as shown in figure 1-1c on day 6. g) Multiple vacuoles (arrows) developed between adjacent ECs of which nucleus were denoted by broken blue circles. h) Capillary-like lumen formation by ECs in vitro. i) ECs were connected to each other by VE-cadherin (red). j-k) Dynamic remodeling of the *in vitro* angiogenesis, which included regression (broken line), growth (becoming thicker) and newly-appearing sprout in the same field for 48h. l-m) GFP-EC tubes aligned with basement membrane stained by type IV collagen. n) A lumenized network of capillaries *in vitro*.

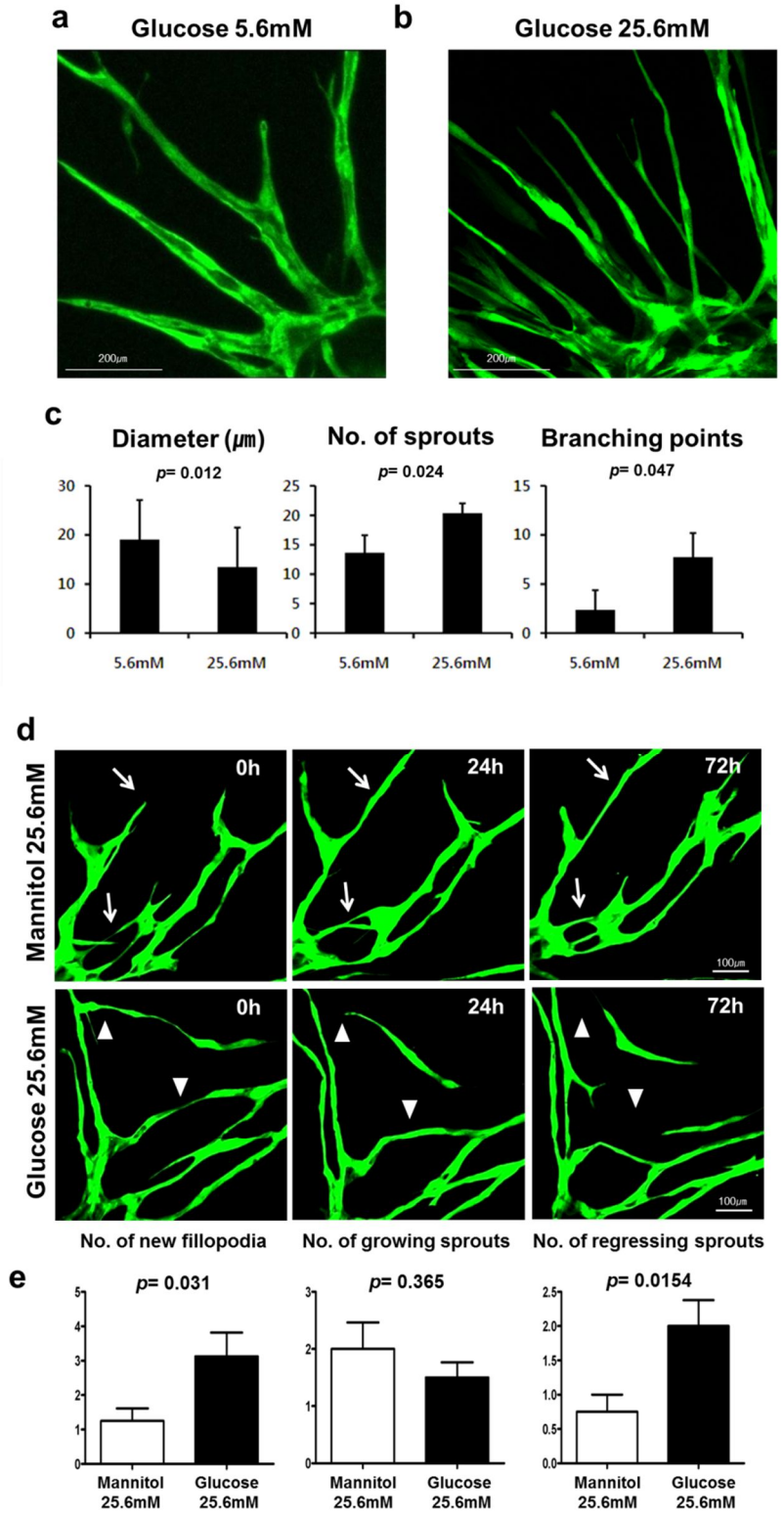
a
Glucose 5.6mM
b
Glucose 25.6mM
200μm
200μm
c
Diameter (μm)
p= 0.012
No. of sprouts
p= 0.024
Branching points
p= 0.047
5.6mM
25.6mM
d
Mannitol 25.6mM
Glucose 25.6mM
0h
24h
72h
100μm
No. of new fillopodia
No. of growing sprouts
No. of regressing sprouts
e
p= 0.031
p= 0.365
p= 0.0154
Mannitol 25.6mM
Glucose 25.6mM

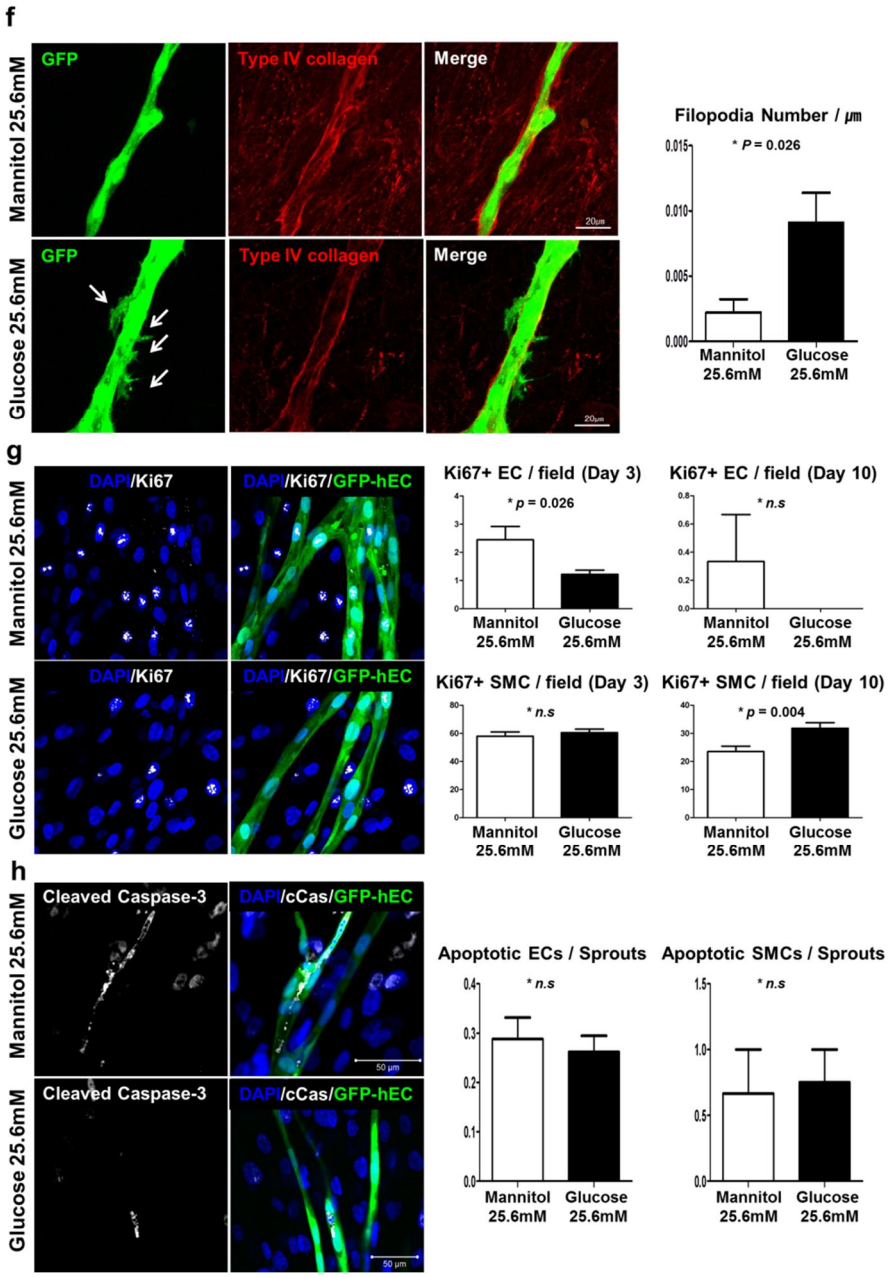

Figure 1-2. Characterization of high glucose-induced abnormal angiogenesis.

a-c) High glucose concentration produced the caliber of tubes narrower and increased filopodia at tip cells, sprouting and

branching more than normal glucose concentration did (n=3). **d)** Active remodeling process (growth and regression) during in vitro angiogenesis in high glucose concentration. Arrow: growing sprouts, arrow head: regressing sprouts. **e)** In contrast to mannitol, high glucose increased the number of new filopodia and regressing sprouts (n=8). **f)** New filopodia from stalk cells through basement membrane (arrow) in a high glucose condition in contrast to stable stalk cells in a mannitol control. High glucose condition significantly increased the number of filopodia per tube length in response to exogenous VEGF ($p=0.026$, n=4). **g)** Ki67 staining to assess cellular proliferation and its quantification in EC and SMC in the model at day 3 and day 10 (n=9). **h)** Cleaved caspase-3 staining to demonstrate apoptosis and its quantification in EC and SMC in the model (n=4).

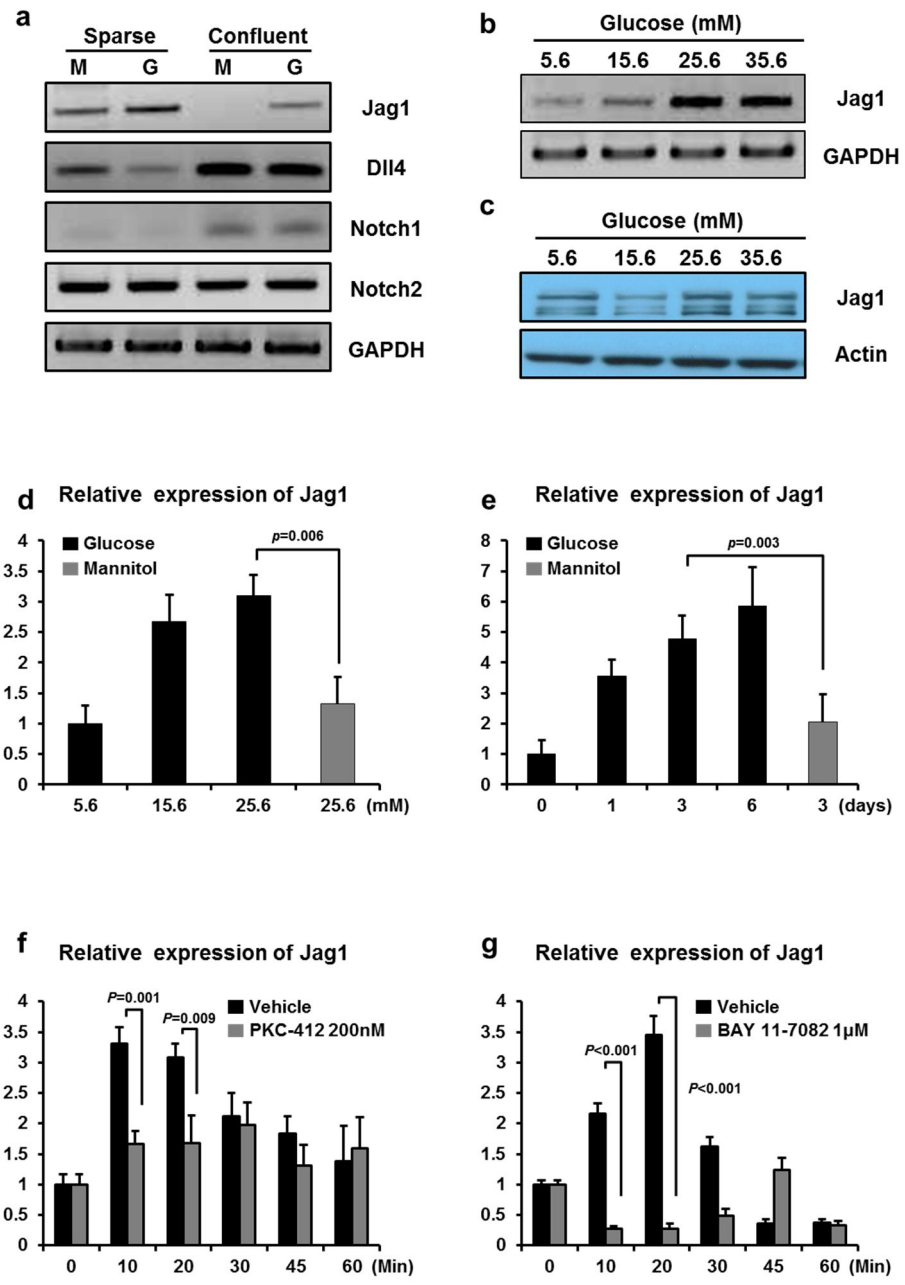
a
Sparse
Confluent
M
G
M
G
Jag1
Dll4
Notch1
Notch2
GAPDH
b
Glucose (mM)
5.6
15.6
25.6
35.6
Jag1
GAPDH
c
Glucose (mM)
5.6
15.6
25.6
35.6
Jag1
Actin
d
Relative expression of Jag1
Glucose
Mannitol
p=0.006
4
3.5
3
2.5
2
1.5
1
0.5
0
5.6
15.6
25.6
25.6 (mM)
e
Relative expression of Jag1
Glucose
Mannitol
p=0.003
8
7
6
5
4
3
2
1
0
0
1
3
6
3 (days)
f
Relative expression of Jag1
P=0.001
P=0.009
Vehicle
PKC-412 200nM
4
3.5
3
2.5
2
1.5
1
0.5
0
0
10
20
30
45
60 (Min)
g
Relative expression of Jag1
Vehicle
BAY 11-7082 1μM
P<0.001
P<0.001
4
3.5
3
2.5
2
1.5
1
0.5
0
0
10
20
30
45
60 (Min)

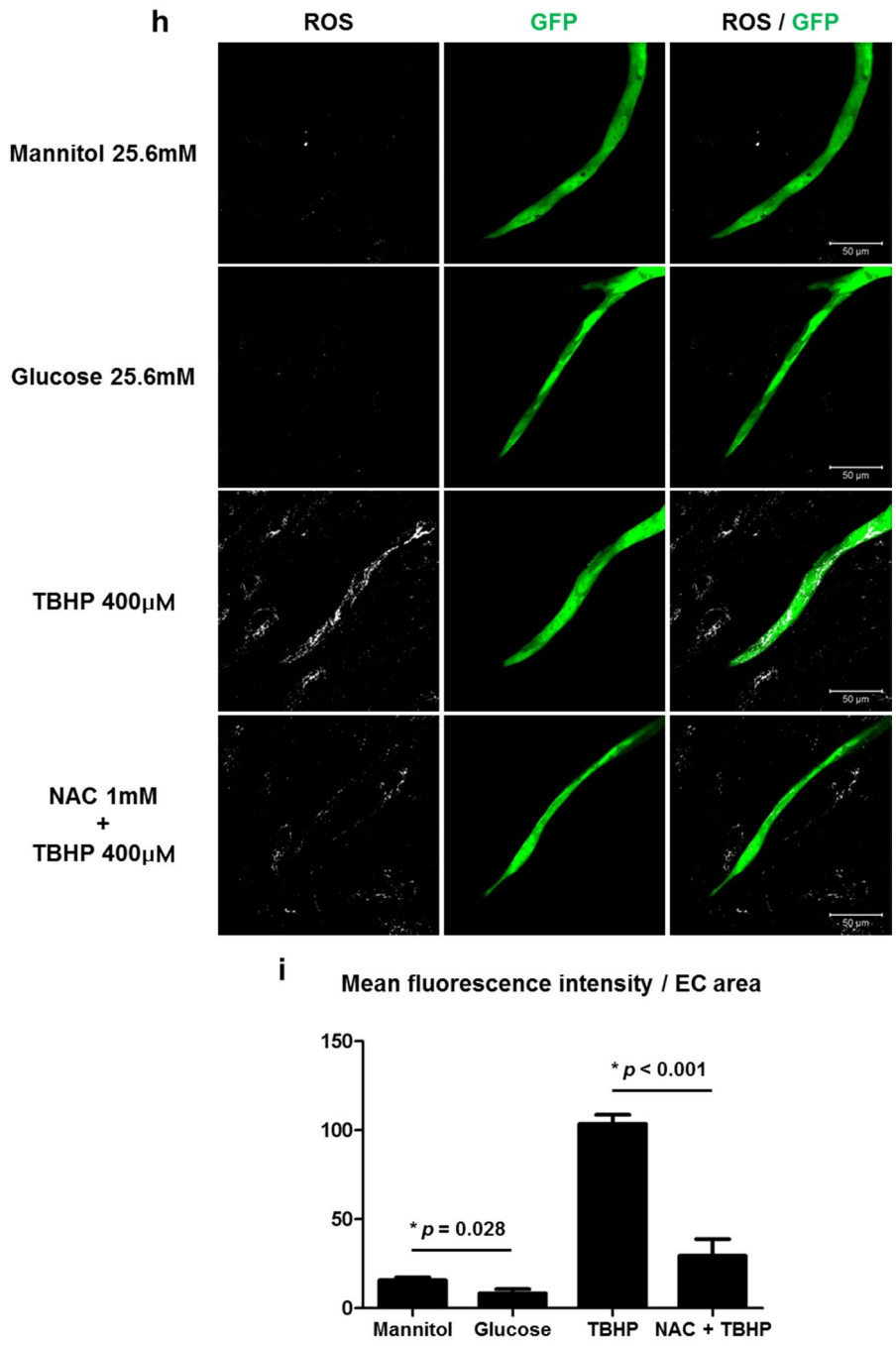

Figure 1-3. Endothelial Jag1 induction and its molecular mechanism by high glucose condition.

a) High glucose (G) increased Jag1 more than mannitol (M) did both in sparse or confluent condition of endothelial cells. Neither Dll4, Notch1 nor Notch2 changed significantly by high glucose. **b,c)** Glucose concentration 25.6mM showed highest Jag1 expression in b) RT-PCR or c) western blot. **d)** Quantitative PCR confirmed that glucose dose-dependently increased Jag1 expression compared to mannitol. (n=4) **e)** High glucose gradually increased endothelial Jag1 expression for several days. **f)** Non-specific PKC inhibitor, PKC-412, significantly attenuated the induction of Jag1 by high glucose (n=3). **g)** NF-kb inhibitor, BAY 11-7082, significantly blocked induction of Jag1 by high glucose (n=3). **h)** ROS detection by fluorescent dye in the *in vitro* model. Positive control, TBHP significantly increased ROS in EC and NAC reduced ROS in EC. **i)** We found that the high glucose condition in this model did not significantly increased ROS.

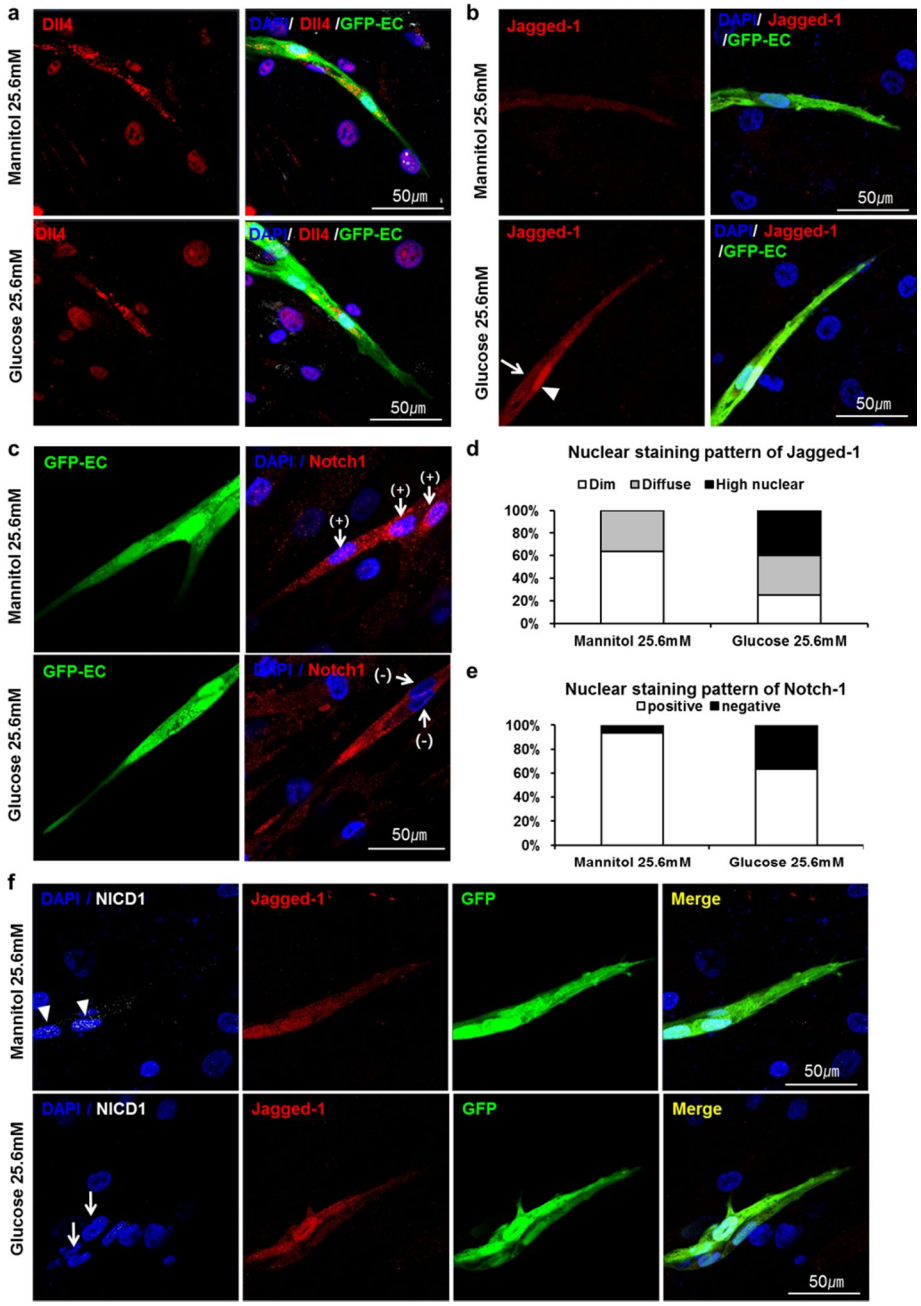

Figure 1−4. High glucose increased Jag1 expression and inhibited Notch signaling in endothelial cells.

a) Dll4 staining showed spotty and perinuclear pattern in ECs. There was no significant difference of Dll4 staining pattern between the two conditions. b) In a high-osmolar control, mannitol condition, ECs showed dim staining of Jag1. High glucose condition increased the intensity of Jag1 expression ('diffuse', arrow) as well as high nuclear enhancement ('high nuclear', arrow head) in ECs. c) In contrast to control, high glucose inhibited nuclear translocation of Notch1 in endothelial nucleus. (+) arrows: Notch1 positive endothelial nucleus, (-) arrows: Notch1 negative endothelial nucleus. . d) High glucose increased 'high nuclear' pattern of Jag1 staining. e) The fraction of cells that are negative for Notch1 nuclear translocation was greater in the high glucose condition than in the mannitol control. f) Mannitol did not decrease NICD nuclear translocation (arrow head) whereas high glucose decreased it, especially in ECs with high nuclear enhancement of Jag1 (arrow).

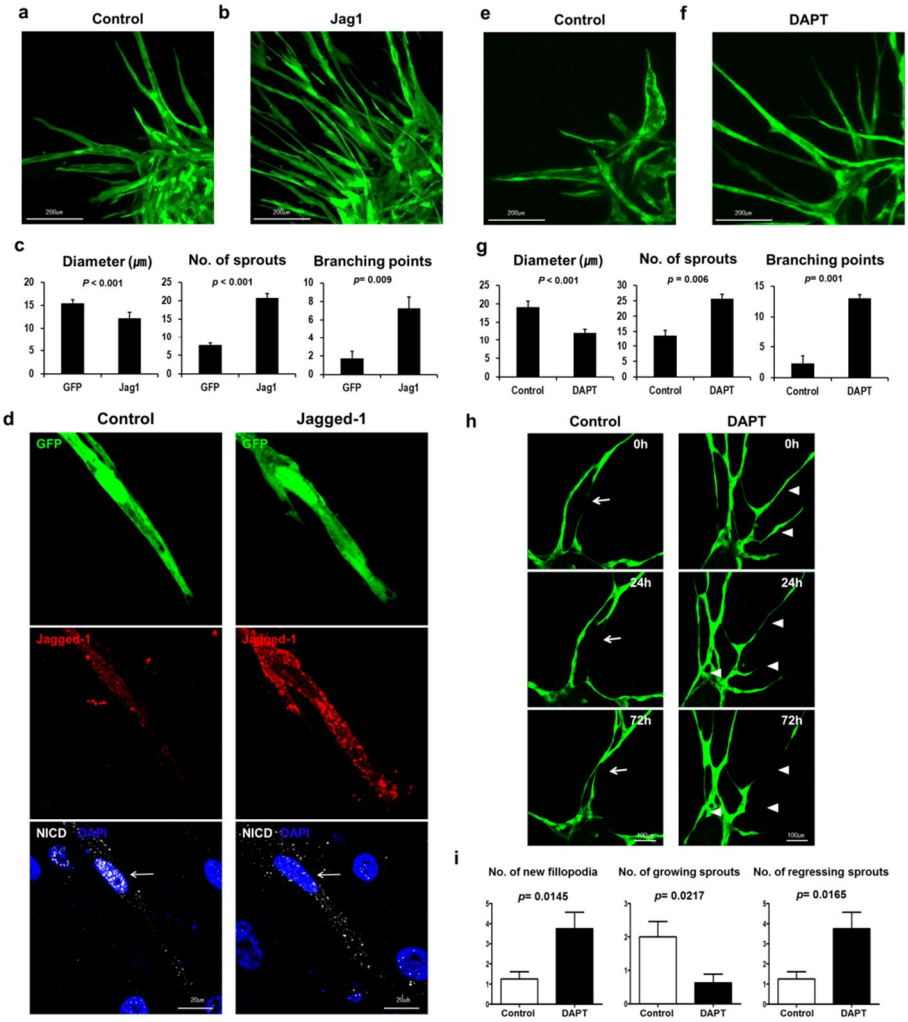

Figure 1-5. Modulation of Notch signaling in *in vitro* model of angiogenesis.

a-b) Sprouting angiogenesis using GFP-ECs or Jag1-overexpressing ECs on day 6. c) Jag1 overexpression showed similar changes to the high glucose condition. n=4, respectively. d) Jag1 overexpression reduced nuclear translocation of Notch1 (white dots in EC nucleus, arrow) compared to the

control suggesting inhibition of Notch signaling in Jag1-overexpressing ECs. **e-f)** Sprouting angiogenesis in control medium and medium with 10 μM DAPT (Notch inhibitor) on day 6. **g)** DAPT reduced diameter of the sprouts and increased sprouting and branching as high glucose condition did. n=4, respectively. **h)** Sequential remodeling of *in vitro* angiogenesis in medium with or without DAPT. Arrow: growing sprouts, arrow head: regressing sprouts. **i)** In contrast to mannitol, DAPT increased the number of new filopodia and regressing sprouts and decreased the number of growing sprouts

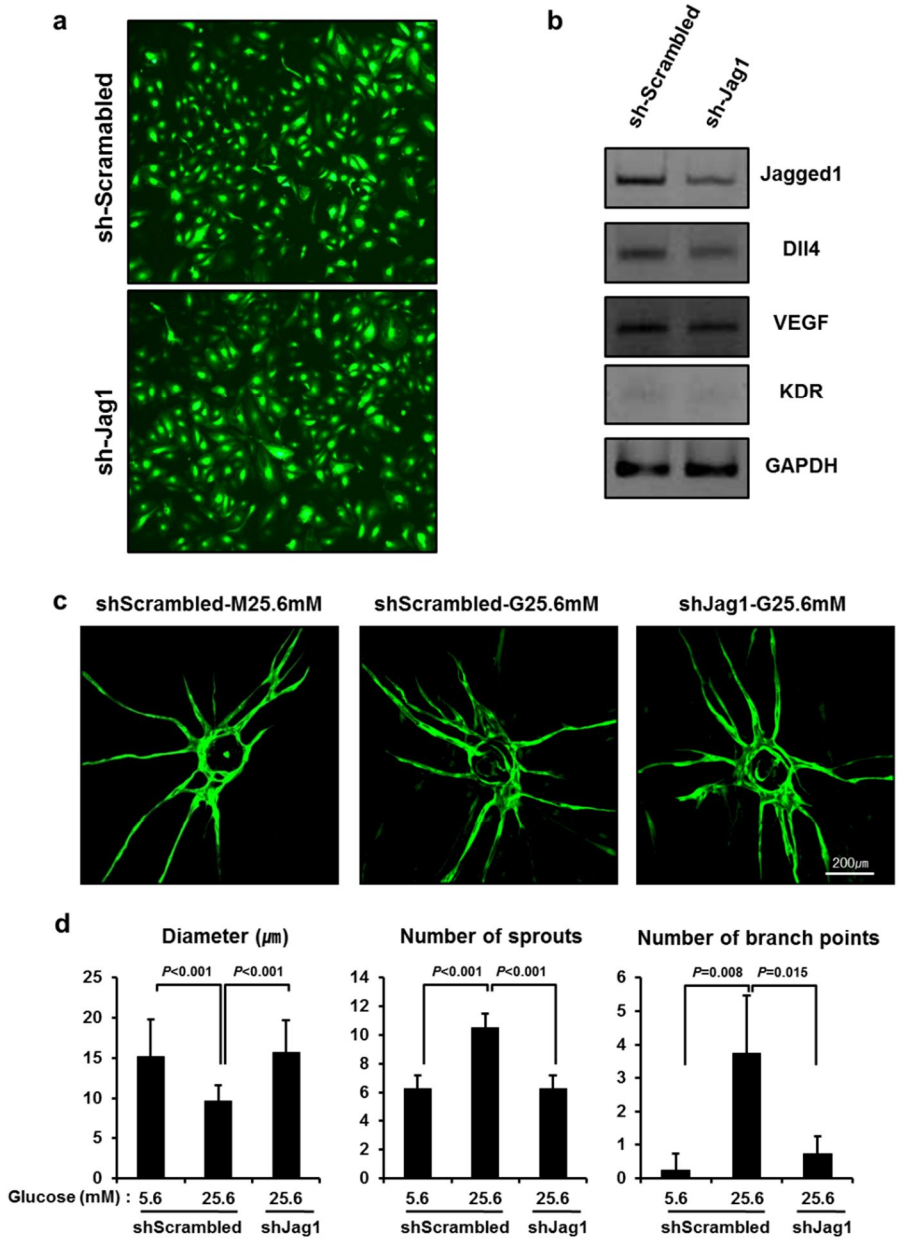

Figure 1-6. Down-regulation of *Jag1* rescued aberrant angiogenesis by high glucose.

a) Lentivirus transduction into ECs for expression of scrambled shRNA or shRNA targeting *Jag1*. b) shRNA targeting *Jag1*

significantly reduced *Jag1* expression in ECs. **c)** Representative figures of spheroid angiogenesis: scrambled shRNA (shScrambled) and normal glucose concentration (G5.6mM), scrambled shRNA and high glucose concentration (G25.6mM), Jag1 shRNA and high glucose, respectively **d)** Quantification data. Jag1 shRNA rescued abnormal sprouting angiogenesis in high glucose condition. (n=4)

DISCUSSION

A novel *in vitro* model of human angiogenesis

Our model has several advantages compared to previous ones. First, we can visualize vessel growth of human ECs without additional staining due to stable fluorescent protein transduction. It was vivid enough to show multiple filopodia of tip cells. This enabled us to observe a real-time vessel growth. Second, this model showed not only sprouting but also tubulogenesis, lumenization, and vascular network formation. This enabled us to reveal the mechanism of vascular stabilization or regression which has not been thoroughly investigated yet. Third, genetic manipulation in this model is relatively easier than that in producing a transgenic animal model. Simple transduction using siRNA, microRNA, or lentiviral vector could reveal the effect of a target gene on angiogenesis. Fourth, if we combine genetic modulation with multicolor labeling, we can dissect even more complex signaling by several genes related to vessel growth. We expect this model to be useful for investigating the various aspects of angiogenesis.

Although a murine retina model may recapitulate in vivo phenomenon in contrast to an in vitro model, we recognized several limitations of the *in vivo* model. First, it is a mouse model which can be different from the human system. Second, since neonatal murine retina model is required to investigate angiogenesis, we need a neonatal murine hyperglycemic model in order to evaluate the effect of high glucose on angiogenesis. However, there is no established neonatal hyperglycemic model as far as we know. Third, we need more time and effort to study various aspects of *in vivo* phenomenon using a mouse model because of the relatively longer breeding time, keeping the animal environment controlled, complex genetic manipulation of the mice, additional staining work, etc. Fourth, if an *in vitro* model can be an alternative to an *in vivo* model, it is ethical to minimize the sacrifice of animals. In these points, our human *in vitro* model has merits. It is a human model. We can control glucose concentration whenever we want. It is easy and fast to reproduce experiments. It is relatively easy to modify genes by transfecting vectors to endothelial cells before making spheroids. It is a good alternative to an *in vivo* system. Therefore, we believe that this model has advantages in

studying human angiogenesis, especially in a hyperglycemic condition.

High glucose-induced abnormal angiogenesis in *in vitro* model of human angiogenesis

Delicate regulation and balance between tip and stalk cells via cell-to-cell signaling are needed during vascular formation. We hypothesized that a disturbance of this signaling resulting in endothelial cell-to-cell miscommunication might be one of the mechanisms of diabetic microvasculopathy. Using our model, we characterized high glucose-induced abnormal angiogenesis which is characterized as heavily-arborized fine tubes as results of increased sprouting, transient growth, and active regression without significant change in EC proliferation and apoptosis. Similar effects by Notch signaling inhibition to the high glucose condition in this angiogenesis model confirmed that high glucose-induced Jag1 overexpression with Notch signaling suppression in ECs resulted in the abnormal angiogenesis. Induction of *Jag1* expression in ECs was known to be mediated by NF-κB which is a downstream molecule of TNF[30]. PKC was also reported to be a mediator of diabetic vasculopathy[15]. We

found that the increased endothelial expression of *Jag1* is mediated by the two well-known DM-related signaling molecules in the present study. Therefore, Jag1 overexpression in ECs is a novel convergence and divergence of a signal pathway from high glucose condition to abnormal angiogenesis.

Modulation of Notch signaling in *in vitro* human angiogenesis model

The Notch signaling pathway is a highly conserved intercellular signaling mechanism that is mediated by interactions between transmembrane ligands and Notch receptors; 5 ligands (Dll1, Dll3 Dll4, Jag1 and Jag2) and 4 Notch receptors (Notch1-4) have been identified in mammals[31]. Among them, two ligands (Dll4 and Jag1) and all four Notch receptors are expressed in the vasculature[25]. Several human and mouse genetic studies suggest that Notch signaling is closely related to proper formation and maintenance of the vascular system[1, 5, 6].

New vessel formation is a dynamic process which involves specification of several types of specialized ECs such as tip, stalk, and phalanx EC, each of which has a distinct function in vessel growth[4, 32]. A previous study implicated Notch signaling

as a key determinant to specify EC phenotypes[5]. Various key molecules and pathways also have been studied in the dynamics of angiogenesis in the context of controlling tip cell selection, sprouting and the formation of new vessels[2]. We found that our model could vividly present the abnormal angiogenesis by visualization of the disturbed behavior of the specialized ECs, which were modulated by Notch signaling. Inhibition of Notch signaling by DAPT increased the number of sprouts and branching points, which were a result of the enhanced tip cell formation. This finding was consistent with a previous report which showed increased sprouts and branching points in retinal angiogenesis of neonatal mice by DAPT administration[5]. We also found that Jag1 overexpression had similar effects to DAPT treatment in this spheroid model of mixed ECs and SMCs. This is consistent with previous reports of the concentration-dependent, ligand-mediated inhibition of Notch signaling. Fiuza et al.[33] showed that ligand can inhibit Notch signaling as a cell autonomous process, which is called as cis-inhibition. In the signal-receiving cells of this study, the overexpressed
Jag1 may bind and inhibit Notch (cis-inhibition) as well as inhibit trans-signal from the signal-sending cells (like Dll4 on

adjacent cells). Yang et al. showed that Notch glycosylation differentially affect signal transduction by Delta-like ligands or Jag1[34]. In line with the above studies, Benedito et al. showed that Notch ligand Jag1 antagonized Dll4-Notch signaling in mice[6]. The mechanism of aberrant vessel growth by elevated Jag1 expression may be due to disequilibrium between the two Notch ligands, Dll4 and Jag1, which showed distinct spatial expression patterns and opposing functional roles regulating angiogenesis.

A novel target to control diabetic microvasculopathy beyond glucose control

It is well known that diabetic vasculopathy, especially microvasculopathy, can be prevented by intensive glucose control[10, 35]. Inversely, it means that the mechanism of microvasculopathy is closely linked to high glucose condition. However, intensive glucose control often causes fatal complication such as hypoglycemia, resulting in the difficulty to achieve the predetermined goal of glucose level even with this strategy[36]. Until now, clinical trials by targeting the previously-proposed pathophysiology of diabetic vasculopathy have failed

to prove therapeutic efficacy, in part because the mechanism of diabetic vasculopathy is too complex and heterogeneous for one to decide a target[14]. Therefore, we need to find a new target which is a bottle neck or a critical step in the mechanism of diabetic microvasculopathy. In that sense, Jag1 or Notch signaling in ECs can be a feasible therapeutic target for diabetic microvasculopathy. In fact, we proved that down-regulation of Jag1 could rescue the abnormal angiogenesis and vascular remodeling in high glucose condition. This could be validated in vivo in a future study.

Limitation

We used a monolayer of SMCs for the culture of EC and SMC spheroids. This system has an advantage for microscopic observation of angiogenesis. However, it has a drawback also. Since cells are co-cultured and RNA and proteins are collected from the mixture of ECs and SMCs, the accuracy of RT-PCR and western blot cannot be assured for a molecular study. To identify the mechanisms of *Jag1* expression in response to glucose levels, we used single cell (EC) culture for the molecular study. The result may not correctly represent the

findings obtained from the co-culture system. Therefore, we used immunofluorescence-imaging study to identify the induction of Jag1 and suppression of Notch signaling in ECs, and used the molecular study of an EC monolayer to confirm it.

In addition, the possibility that DAPT or high glucose affected SMCs in the model may not be excluded. This is because Notch signaling regulates differentiation of SMCs as well. In return, altered SMC function might affect EC angiogenesis. However, EC-specific Jag1 over-expression or down-regulation showed similar changes to the one by treatment of DAPT or high glucose. Therefore, we believe that the abnormal angiogenesis in high glucose condition is probably caused by the disturbed Jag1/Notch signaling in ECs.

The significance of this study representing diabetes is limited as we only used glucose in vitro. Further study using a diabetic animal model or human tissue may reveal a pathogenic role of Notch signaling in diabetic vasculopathy.

In conclusion, a novel in vitro model of human angiogenesis is a useful tool for investigating the mechanism of physiologic and pathophysiologic angiogenesis and vascular remodeling. Specifically, high glucose condition induced Jag1 and

suppressed Notch signaling in ECs, which suggests that Jag1/Notch would a promising therapeutic target of diabetic microvasculopathy.

In summary, we characterized abnormal angiogenesis in high glucose condition using a novel in vitro angiogenesis model using co-cultivation of ECs and SMCs in a spheroid on an SMC monolayer. It was mediated by Jag1 overexpression and Notch signaling inhibition in ECs. Suppression of Jag1 could rescue the aberrant angiogenesis (Figure 1-7).

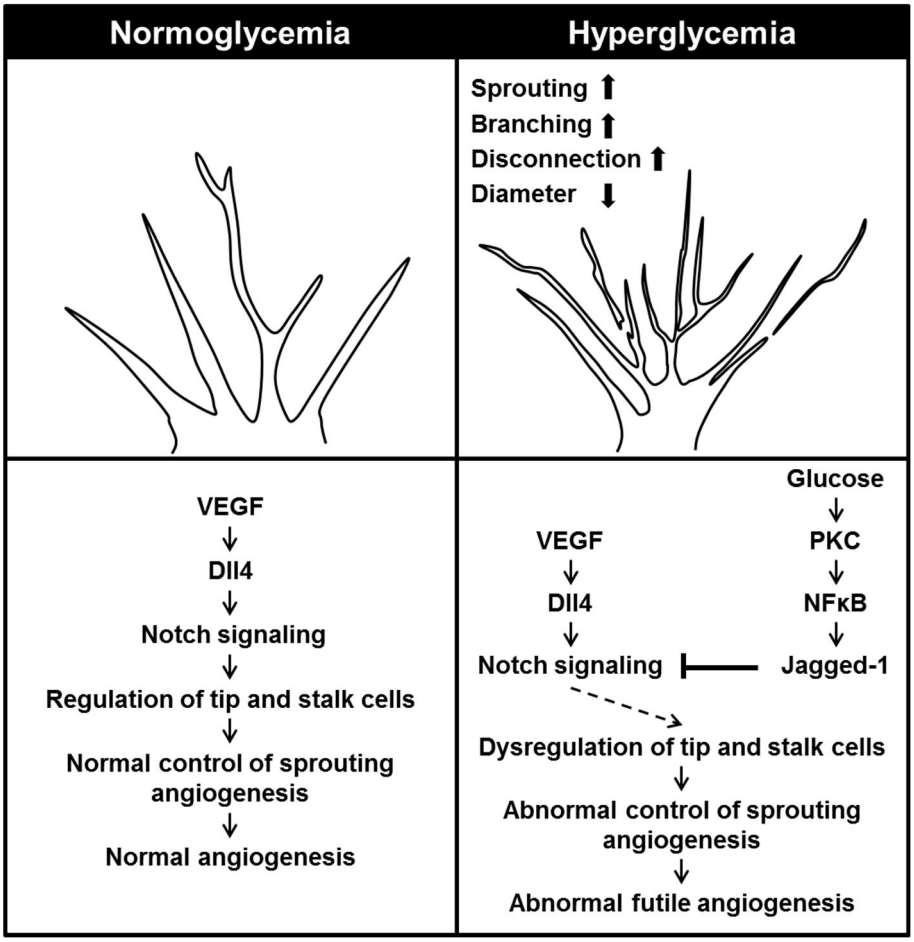

Figure 1-7. Scheme of the aberrant angiogenesis induced by Jag1 overexpression under high glucose condition in the *in vitro* model of human angiogenesis.

CHAPTER 2

Hyperglycemia–induced Jagged1 overexpression in endothelial cells causes retinal capillary regression in a murine model of diabetes mellitus: Insights into diabetic retinopathy

INTRODUCTION

Hyperglycemia, a major risk factor for diabetic microvascular complications, induces apoptosis in retinal pericytes, renal podocytes, and vascular endothelial cells (ECs) directly or indirectly through inflammation, oxidative stress, glycated products, or protein kinase C activation[14, 15]. Although intensive glucose control in diabetic patients can delay the onset and progression of diabetic vascular complications[11, 37], clinicians have frequently failed to effectively prevent the progression of vascular diseases, including retinopathy, amongst others, which necessitates further investigation into novel mechanisms of diabetic vasculopathy[35].

Recent advances in vascular biology have revealed that intercellular signaling between adjacent ECs has important roles in development, remodeling, and homeostasis of vessels[2]. ECs in the capillaries are not static but dynamically changed by intercellular signaling[8]. Notch receptors and their ligands, delta-like ligand 4 (Dll4) and Jagged1 (Jag1), regulate the dynamic and transient intercellular signaling between ECs. Once the Notch extracellular domain of one cell interacts with the

Dll4 in adjacent cell, γ-secretase cleaves Notch, thereby releasing the Notch intracellular domain (NICD), which subsequently regulates gene expression via activation of transcription factors. Expression of Dll4 in filopodia-extending ECs (tip cells) leads to the activation of Notch in adjacent ECs, and induces stable tube-forming ECs (stalk cells) at the base of sprouts[5]. The vessel-stabilizing activity of the Dll4-Notch interaction is opposed by Jag1, which destabilizes stalk cells and leads to the immature vessel plexus[6].

Acellular capillaries (e.g., empty basement membrane sleeves or ghost vessels) have been reported to be an irreversible result of hyperglycemia-induced endothelial cell apoptosis[15]. Acellular capillaries are also observed during developmental angiogenesis in the mouse retina, which is tightly regulated by intercellular signaling via Notch and its ligands[2]. In addition, endothelial glucose metabolism affects developmental angiogenesis by modulating Notch signaling[38] which is crucial for the remodeling of veins and the perivenous capillary plexus after the initial angiogenic growth phase in the postnatal retina[39]. Therefore, it is likely that Notch signaling has a role in adult

vascular homeostasis and is affected by dysregulated glucose metabolism.

However, Notch signaling and vascular remodeling in mature adult capillaries has not yet been fully investigated, especially in relation to hyperglycemia. We demonstrate that abnormal intercellular Notch signaling has a crucial effect on diabetic microvasculopathy in the present study.

MATERIALS AND METHODS

1. Mice

All animal experiments were approved by the Institutional Animal Care and Use Committee (IACUC). Diabetes mellitus (DM) was induced in 8-week-old male C57BL/6 mice by intraperitoneal (i.p.) injection of 150 mg/kg streptozotocin (STZ; Sigma Aldrich, St. Louis, MO, USA) dissolved in citrate buffer. Blood glucose levels were measured every week after STZ administration. Induction of diabetes was defined in mice when their non-fasting blood glucose levels were greater than 250 ㎎/㎗. HbA1c levels were determined using the HITACHI 7070 automatic biochemical analyzer (Hitachi Instruments, Tokyo, Japan) at 6 weeks after STZ injection. Eyes, hearts and thigh muscles were harvested 6 weeks after induction of diabetes and compared to a control group. To elucidate the role of Jag1 in ECs, we used both EC-specific *Jag1* heterozygous deficient (*Tie2-Cre+;Jag1*$^{flox/+}$) mice and EC-specific inducible *Jag1* deficient (*Tie2-CreER*^{T2}*+;Jag1*$^{flox/flox}$) mice. *Jag1*$^{flox/+}$ mice were purchased from Jackson Laboratories (Bar Harbor, ME, USA). *Tie2-Cre* mice were kindly provided by Dr. Gou Young

Koh (Korea Advanced Institute of Science and Technology, Daejeon, South Korea). *Tie2-CreER*^{T2} mice were a generous gift from Dr. Stefan Offermanns (Max Plank Institute, Bad Nauheim, Germany). For comparison, *Tie2-Cre+;Jag1*$^{flox/+}$ mice and *Tie2-Cre+;Jag1*$^{+/+}$ litter-mate controls were examined in the same experiments.

To confirm that Notch inhibition led to retinal microvasculopathy (RM), we generated conditional *Mib1* knockout mice under the control of an inducible *Tie2* promoter. *Mib1*$^{flox/flox}$ mice were kindly provided by Dr. Young-Yun Kong (School of Biological Science, College of Natural Sciences, Seoul National University, Seoul, South Korea). *Tie2-CreERT2+;Mib1*$^{flox/+}$ mice received i.p. injection of 1 ㎎ 4-OHT-tamoxifen for 7 consecutive days from 8 weeks after birth. We harvested retinas at 10 weeks after birth. Pharmacological Notch inhibition was achieved by intraperitoneal injection of a gamma secretase inhibitor (GSI), 100 ㎎/㎏ DAPT (N-[N-(3,5-difluorophenacetyl-L-alanyl)]-S-phenylglycine tert-butyl ester, Sigma Aldrich) for 3 consecutive days prior to harvesting. We also used another

GSI, dipeptidic DBZ. We injected DBZ intraperitoneally at a dosage of 10 ㎛㏖/㎏ every other day for 4 weeks.

2. Immunofluorescence staining and confocal microscopic analysis

Mice were anaesthetized and perfused with 30 ㎖ of PBS via the left ventricle. The eyes were enucleated and fixed in 2% paraformaldehyde (PFA) in PBS for 45 minutes at room temperature. Retinas were dissected, permeabilized with 1% bovine serum albumin (BSA) in 0.5% Triton-X100 (Sigma Aldrich) overnight at 4℃, and incubated with tetramethyl rhodamine isothiocyanate (TRITC)-conjugated Bandeiraea simplicifolia (BS)1-lectin (Sigma Aldrich, St. Louis, MO, USA) overnight at 4℃. For further investigation, the retinas were stained overnight at 4℃ with specific primary antibodies: anti-Jag1 (Santa Cruz Biotechnology, Santa Cruz, CA, USA; Abcam, Cambridge, UK), anti-Dll4 (Santa Cruz Biotechnology, Santa Cruz, CA, USA), anti-Notch1 (Cell Signaling Technology, Danvers, MA, USA), anti-cleaved Notch1 (Cell Signaling Technology, Danvers, MA, USA; Abcam, Cambridge, UK), anti-

type IV collagen (Southern Biotechnology Associates, Birmingham, AL, USA; Abcam, Cambridge, UK), anti-VE-cadherin (Santa Cruz Biotechnology, Santa Cruz, CA, USA), anti-N-cadherin (Santa Cruz Biotechnology, Santa Cruz, CA, USA), anti-HEY-1 (Abcam, Cambridge, UK), anti-NG2 (Millipore, Billerica, MA, USA), anti-ZO1 (Invitrogen, Carlsbad, CA, USA), anti-VEGFR2 (R&D Systems, Weisbaden, Germany), and anti-VEGFR3 (R&D Systems, Weisbaden, Germany) followed by incubation with fluorescently tagged secondary antibodies (Invitrogen, Carlsbad, CA, USA) overnight at 4℃. For heart and thigh muscles, the isolated tissues were embedded in optimal cutting temperature compound (OCT; Tissue-Tek, USA) and stored in a −80℃ deep freezer. Frozen sagittal sections were cut at 25-30 μm using a cryostat (HM 550 MP, Microm; Walldorf, Germany). The sections were fixed with 4% PFA in PBS for 10 minutes and permeabilized with 10% fetal bovine serum (FBS), 0.5% Triton-X100 in PBS for 4-6 hours, followed by primary and secondary antibodies incubations for 2-3 days each at 4℃. The images were acquired by a confocal laser scanning microscope system (LSM 710, Carl Zeiss AG, Oberkochen, Germany) and processed with

Zen2008 software (Carl Zeiss AG, Oberkochen, Germany) and ImageJ (NIH, MD, USA) software. A water- or oil-immersion objective (40× or 63×, 1.4 numerical aperture) with the pinhole set for a section thickness of 0.8-1.2 ㎛ (1 airy unit in each channel) was used. To visualize the three-dimensional reconstructed image, a Z-stack of 20 ㎛ thickness was obtained. Diode 405 ㎚, Multi-Argon 488 ㎚, HeNe 543 ㎚, and HeNe 633 ㎚ laser lines were selected, and images were sequentially acquired using separate laser excitations to avoid cross-talk between different fluorophores.

3. Immunofluorescence quantification of retinal vasculopathy and statistical analysis

Images were generated for comparative analysis under identical conditions of light, contrast, and magnification. Capillary density, diameter, and mean fluorescence intensity were measured by ImageJ software (NIH, MD, USA). This program automatically detects signal pixel area. If the staining is very specific, i.e., the signal-to-noise ratio is high, the capillary area tends to be low. If the staining is not very specific, the capillary area becomes

high because noise is included in the area. We performed BS-1 lectin staining for each set of experiments at the same time. However, it is hard to compare the results between the different sets of experiment in the present study because of staining variation.

We directly evaluated the capillary diameter at various points of interest in z-stack images by measuring the width of the lectin-positive area perpendicular to the capillary length using ImageJ software. Therefore, the capillary diameter in our data denotes the abluminal diameter of the capillary, but not luminal diameter. We counted a capillary as acellular if the diameter of the lectin-stained structure was markedly different from the adjacent capillaries, and did not contain a nucleus.

All results are expressed as mean ± standard error of mean (SEM). Differences in continuous variables between experimental groups were analyzed by Student's t-test using GraphPad Prism 5 (GraphPad Software, San Diego, CA, USA).

4. Apoptosis and proliferation analysis

For examining cell proliferation, BrdU (BD Pharmingen, San Diego, CA, USA) was administered for two consecutive days

prior to harvest at a dose of 50 ㎎/㎏ i.p. The eyes were enucleated and fixed in 2% PFA for 45 minutes at room temperature followed by retinal dissection in PBS. Following incubation in a blocking solution (1% BSA, 0.5% Triton X-100 in PBS) overnight at 4℃, retinas were placed in 2N HCl for 30 minutes at room temperature and washed twice in 0.2 M sodium borate for 15 minutes. The retinas were then incubated with a FITC-conjugated anti-BrdU antibody (eBioscence, San Diego, CA, USA) overnight at 4℃.

Retinal cell apoptosis was determined by a terminal deoxynucleotide transferase nick end labeling (TUNEL) assay using an in situ cell death detection kit (Roche Diagnostics, Mannheim, Germany). The total number of TUNEL-positive cells was counted in each retina. Retinal cell death was also measured by flow cytometry with an Annexin V-FITC Apoptosis Detection Kit (BD Bioscience, Franklin Lakes, NJ). Retinas were digested in Accumax (Millipore, Billerica, MA, USA) and retinal cell apoptosis was assessed by annexin V binding by flow cytometry (FACSAriaⅢ, BD Bioscience, San Jose, USA).

5. Genotyping and Reverse transcription-polymerase chain reaction (RT-PCR)

Genomic DNA extraction from a mouse tail biopsy and polymerase chain reaction (PCR) were performed using REDExtract-N-Amp Tissue PCR kit (Sigma Aldrich, St. Louis, MO, USA) with the following primers: 5′-TCAGGCATGATAAACCCTAGC-3′, 5′-CTACATACAGC-ATCTACATGC-3′ for *Jag1*$^{flox/+}$ mice; 5′-GCGGTCTGGCA-GTAAAAACTATC-3′, 5′-GTGAAA-CAGCATTGCTGTC-ACTT-3′ for *Tie2-Cre* mice; 5′-GAA-GTCGCAAAGTT-GTGAGTTG-3′, 5′-TGGCTTGCAGGTACAGGA-3′, 5′-GAGAATGGCGAGAAGTCACTG-3′ for *Tie2-CreER*^{T2} mice. To verify the efficiency and specificity of Cre recombinase activity, aortic ECs were isolated by enzymatic digestion. The inside of the aortic lumen was washed with PBS and filled with 0.1% type II collagenase (Gibco, Carlsbad, CA, USA) in PBS through a 24-gauge catheter (BD, Franklin Lakes, NJ, USA). After incubation for 10 minutes at 37℃, ECs were collected by flushing with 2 ㎖ of EC growth media EGM-2MV (Lonza, Verviers, Belgium) and plated on culture dishes coated with 1.5%

gelatin (Sigma Aldrich, St. Louis, MO, USA). After removal of ECs, SMCs were subsequently isolated. The remaining tissue was cut into pieces and digested with 0.5% collagenase for 4 hours at 37℃ in a shaking incubator, followed by collecting and culturing of cells in low-glucose DMEM containing 10% FBS (Gibco, Carlsbad, CA, USA). For reverse transcriptase (RT)-PCR, total RNA was isolated from cultured ECs using an RNeasy Mini Kit (Qiagen, Valencia, CA, USA). Reverse transcription was performed using 1 ㎍ of RNA with amfiRivert cDNA synthesis premix (GenDepot, Barker, TX, USA). cDNA was PCR-amplified using EX Taq (TaKaRa, Kyoto, Japan) and the following primers: 5′ -CGACCGTAATCGCATCGTAC-3′ and 5′ - AGTCCCACAGTAATTCAGATC-3′ for the flanked exon 4 of *Jag1*. The upper band (541 bp) indicates that the wild-type allele is present. The lower bands (286 bp) indicate the *Jag1* mutant allele that does not contain exon 4.

6. *In vitro* angiogenesis model using hEC and hSMC

ECs were transduced with shRNA and eGFP expressing lentiviral vector. Mixture of transduced ECs and non-labeled SMCs were suspended in EGM (Lonza, Basel, Switzerland)

containing 20% MethoCult (Stem Cell Technologies Inc., Vancouver, BC, Canada) and then spheroidal cell aggregates were formed in conical-bottom 96-well plates (Nunc, Wiesbaden, Germany). After 24 hours, mixed cell spheroids were seeded on monolayer cultured SMCs. We utilized the lentiviral vector, pLentiLox 3.7 (pLL3.7), to deliver shRNA targeting endogenous Mib1: 5' - CCTCTGGGATAATGGTGC-3'. A scrambled sequence, 5' - CAACAAGATGAAGAGCAC-CAA -3', was used as a negative control.

RESULTS

Characterization of hyperglycemic retinal and myocardial vasculopathy in adult mice

We induced hyperglycemia in mice by intraperitoneal administration of 150 mg/kg STZ. Blood glucose levels were maintained higher than 400 mg/dL and the HbA1c level was 7.2% at six weeks. At this point, we identified RM. In the hyperglycemic mice, capillary area and capillary diameter were significantly decreased (Figure 2-1a,b). These changes were more prominent in the peripheral retinal region than in the central region near the optic disc. Therefore, we performed further analysis in the peripheral retinal region. We separately analyzed the three layers of the retinal capillaries: superficial, intermediate, and deep, according to their proximity to the vitreous body (Figure 2-1c). Compared to normal mice, hyperglycemic mice showed a marked decrease in capillary density (percent capillary area/retinal area; Figure 2-1d,e). Acellular capillaries were markedly increased in hyperglycemic mice, especially in the deep layer (Figure 2-1f). In addition, the diameter of the intact capillaries with lumens was narrower

in hyperglycemic mice than normal controls (Figure 2-1g). In addition, we observed two different acellular capillaries: regressing vessels having thick type IV collagen deposition and growing ones having thin or no type IV collagen lining (Figure 2-1h). Therefore, we surmised that hyperglycemia increased dynamic capillary remodeling and regression leading to decreased capillary density in adult mice.

Hyperglycemia-induced Jag1 overexpression in endothelial cells of retina and myocardium

Two Notch ligands (Dll4 and Jag1) are expressed in the vasculature[25]. Jag1 was highly expressed in the hyperglycemic retinal capillaries compared to those in controls (Figure 2-2a). Jag1 signal intensity in ECs markedly increased in the hyperglycemic mice (Figure 2-2b). Jag1 in the capillaries of hyperglycemic heart, skeletal muscle, and glomerulus of the kidney was also upregulated. We confirmed Jag1 overexpression in response to the high glucose condition in human umbilical vein endothelial cells by western blot. In contrast to Jag1, no difference in Dll4 expression was observed between hyperglycemic mice and the controls.

Knockdown of *Jag1* prevented retinal microvasculopathy in diabetic mice

To evaluate whether endothelial Jag1 overexpression is the primary mechanism for hyperglycemia-induced RM, we assessed the effect of hyperglycemia in endothelial-specific *Jag1* knockdown mice, *Tie2-Cre*+;$Jag1^{flox/+}$. We confirmed the endothelial-specific knockdown of *Jag1* in isolated ECs from these mice (Figure 2-3a). In the normoglycemic condition, *Tie2-Cre*+;$Jag1^{flox/+}$ mice did not display any capillary abnormality compared to *Tie2-Cre*+;$Jag1^{+/+}$, wild-type mice (Figure 2-3b,c). Hyperglycemic wild type mice (*Tie2-Cre*+;$Jag1^{+/+}$) developed apparent RM. However, knockdown of *Jag1* in ECs as in *Tie2-Cre*+;$Jag1^{flox/+}$ mice markedly attenuated RM even under hyperglycemic conditions (Figure 2-3b,c).

Hyperglycemic retinal vasculopathy can be reversed by *Jag1* knockdown in endothelial cells

To confirm that the established RM was reversed by modulation of Jag1, i.e., whether RM could be treated and cured, we

suppressed Jag1 expression in ECs at 4 weeks after hyperglycemia induction using an inducible knockdown model: *Tie2−CreER*^{T2}+;*Jag1*$^{flox/flox}$ mice. We confirmed that RM was established at 4 weeks after hyperglycemia induction (Figure 2−4a,b). Starting from 4 weeks after hyperglycemia induction, we administered 4−OH tamoxifen (OHT) or vehicle for 7 days (Figure 2−4c). Endothelial−specific inducible knockdown of *Jag1* was confirmed in isolated ECs from the mice (Figure 2−4d). We evaluated the efficiency of *Tie2−CreER*^{T2}−mediated recombination using *Rosa26−eYFP* mice. eYFP expression was observed at about 60% of endothelial cells. Inducible knockdown of *Jag1* in *Tie2−CreER*^{T2}+;*Jag1*$^{flox/flox}$ normoglycemic mice receiving OHT did not produce a different capillary phenotype. Whereas hyperglycemic *Tie2−CreER*^{T2}+;*Jag1*$^{flox/flox}$ mice (STZ group) showed vivid RM in the retina compared to control (Figure 2−4e,f), knockdown of *Jag1* at 4 weeks after hyperglycemia induction by treatment with OHT (OHT group) markedly reversed the established RM during the next 4 weeks compared to the STZ group. Immunofluorescent staining of Jag1 confirmed the downregulation of Jag1 in the STZ+OHT group in contrast to

the STZ+vehicle group (Figure 2-5a,b). This result supports the observation that downregulation of Jag1 can rescue capillary regression and vascular remodelling under high-glucose conditions.

Hyperglycemia decreased Notch signal activity, which was prevented by *Jag1* knockdown in endothelial cells of myocardium as well as retina.

To examine the downstream of Jag1 induction by hyperglycemia, we assessed the signal activity of Notch1 using immunofluorescent staining of full-length Notch1 and NICD1.

Notch1 expression was diffuse, with a salt-and-pepper appearance in neuronal cells and ECs in the retinas of adult mice. NICD1 staining displayed a similar pattern to that of full-length Notch, but relatively higher signaling in the nucleus of ECs than in neuronal cells. To quantify endothelial-specific levels of Notch1 and NICD1 expression, we cropped the Notch1 or NICD1 signal within ECs or endothelial nuclei. Next, we quantified the signal intensity of Notch1 or NICD1.

Endothelial Notch1 expression was not substantially different between normoglycemia and hyperglycemia in the retina and

heart (Figure 2-6a,b,c). By contrast, NICD1 signal intensity was markedly lower in the hyperglycemic ECs of retina, heart, and skeletal muscle than in normoglycemic ones, which suggests that hyperglycemia inhibits Notch1 signaling in ECs (Figure 2-6d,e,f). A downstream molecule of NICD1, HEY1 was also significantly decreased in the hyperglycemic myocardial endothelial cells (Figure 2-6g,h). Endothelial-specific knockdown of *Jag1* did not affect Notch1 expression in the hyperglycemic mice (Figure 2-6i,k). In contrast, it significantly recovered NICD1 (Figure 2-6j,l). This suggests that the decrease of NICD1 is mediated by Jag1 upregulation in the hyperglycemic condition and NICD1 can be restored by inhibiting Jag1 upregulation. Similarly, endothelial-specific inducible knockdown of *Jag1* at 4 weeks after hyperglycemia induction did not change Notch1 expression whereas it significantly increased NICD1 suggesting that the decrease of NICD1 was reversed by Jag1 knockdown in the hyperglycemic condition (Figure 2-6m,n).

Chemical inhibition of Notch signaling phenocopied hyperglycemia-induced capillary abnormality.

To confirm whether Notch inhibition induces retinal capillary regression in adults, we introduced the chemical Notch inhibitor, DAPT via intraperitoneal injection. Chemical Notch inhibition phenocopied the capillary changes in hyperglycemic mice and induced RM in normal mice (Figure 2-7a,b). Another chemical Notch inhibition using DBZ also showed similar changes to the hyperglycemic RM and DAPT inhibition (Figure 2-7c,d).

Hyperglycemia and inhibition of Notch signaling decreased endothelial junctional molecules

We also used an additional genetic model of endothelial Notch inhibition using *Tie2-CreER*^{T2}+;*Mib1*$^{flox/+}$ transgenic mice with or without OHT administration. Again, the inducible Notch inhibition with OHT administration induced retinal RM in this genetic model (Figure 2-8a,b).

Next, we investigated whether the endothelial junction is affected by Notch inhibition to demonstrate a possible mechanism of RM. In *in vitro* culture, endothelial tubes showed well organized cell-to-cell junctions by VE-cadherin in the presence of intact Notch signaling (Figure 2-8c). However, VE-cadherin was downregulated by inhibition of Notch

signaling using shRNA against *Mib1* (Figure 2-8d). Likewise, C57BL/6 control mice showed higher expressions of VE-Cadherin and N-cadherin in the retinal endothelial cells than in hyperglycemic C57BL/6 mice (Figure 2-8e,g). We also investigated whether Notch inhibition affected VE-cadherin and N-cadherin using *Tie2-CreER*^{T2}+;*Mib1*$^{flox/+}$ transgenic mice. Endothelial specific-inducible *Mib1* knockdown significantly reduced those adhesion molecules compared to control mice (Figure 2-8f,h).

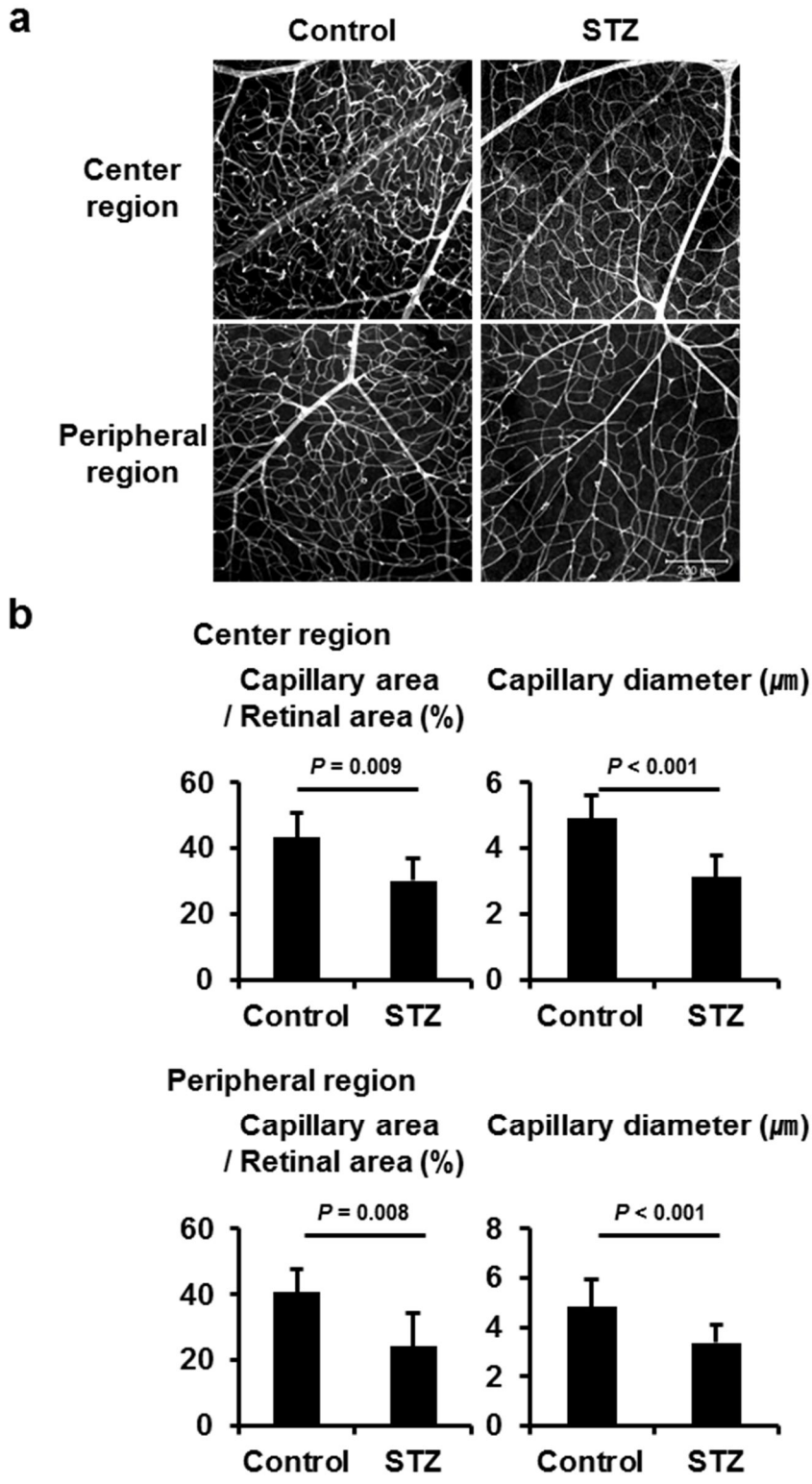
a
Control
STZ
Center region
Peripheral region
b
Center region
Capillary area / Retinal area (%)
Capillary diameter (μm)
P = 0.009
P < 0.001
60
40
20
0
6
4
2
0
Control
STZ
Peripheral region
Capillary area / Retinal area (%)
Capillary diameter (μm)
P = 0.008
P < 0.001
60
40
20
0
8
6
4
2
0
Control
STZ

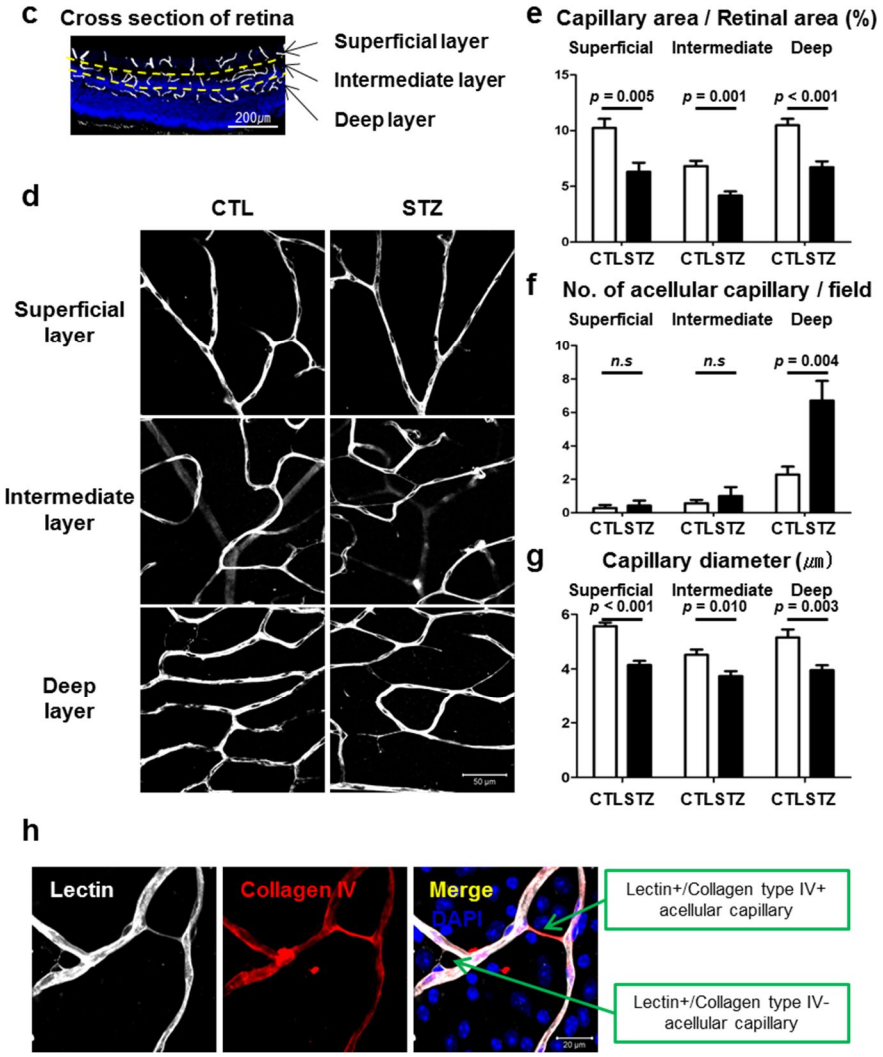

Figure 2-1. Characterization of hyperglycemic retinal vasculopathy in adult mice.

a) Whole-mounted retinas with lectin staining of STZ-induced hyperglycemic C57BL/6 mice showed a reduction of capillary density and diameter in both central and peripheral regions compared to normoglycemic retinal controls. b) Quantification

of retinal capillary density and diameter in control and STZ mice (n = 6 for each group). Capillary density is expressed as the percentage of the BS-1 lectin-stained area and capillary diameters were evaluated by measuring the width of the lectin-positive area perpendicular to the capillary length using ImageJ software. c) A cross-section displayed three vascular layers of the adult retina: the superficial, intermediate, and deep, according to the proximity from the vitreous fluid. Yellow dashed lines delineate the borders of the retinal layers. d) Whole-mounted retinas of STZ mice displayed a reduction of capillary density and an increase of acellular capillaries across all three retinal layers compared to control mice. e-g) Quantification of retinal capillaries in control and STZ mice. STZ mice showed reduced density of retinal capillaries in all three retinal capillary layers (n = 7 for each group). A marked increase in the number of acellular capillaries was observed in the deep retinal layers of the STZ mice (n = 7 for each group). Additionally, a decrease in capillary diameter was also observed in STZ mice (n = 9 for each group). h) Immunofluorescence staining for type IV collagen (red), BS-1 lectin (white), and DAPI (blue) of whole-mounted mouse retinas. Two different

types of acellular capillaries were present, according to the patterns of type IV collagen: one with thick type IV collagen deposition (presumably a regressing vessel); and the other with thin or no type IV collagen lining, (possibly a growing or sprouting vessel).

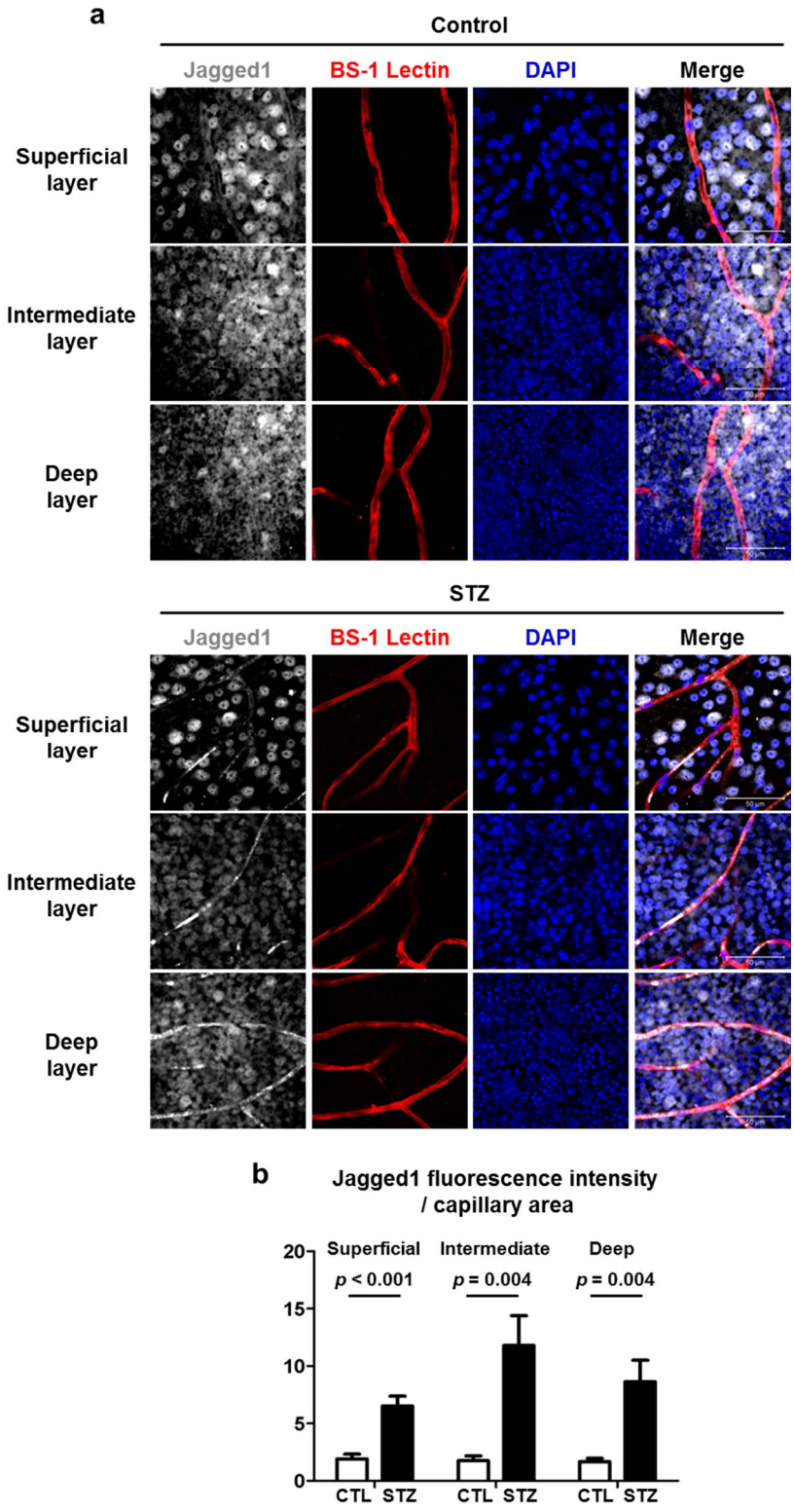
a
Control
Jagged1
BS-1 Lectin
DAPI
Merge
Superficial layer
Intermediate layer
Deep layer
STZ
Jagged1
BS-1 Lectin
DAPI
Merge
Superficial layer
Intermediate layer
Deep layer
b
Jagged1 fluorescence intensity / capillary area
20
15
10
5
0
Superficial
Intermediate
Deep
p < 0.001
p = 0.004
p = 0.004
CTL
STZ
CTL
STZ
CTL
STZ

Figure 2-2. Hyperglycemia-induced Jag1 in endothelial cells.

a) Immunofluorescence staining of Jag1 (white), BS-1 lectin (red), and DAPI (blue) in adult whole-mounted mouse retinas. In control mice, Jag1 expression is observed in most of the retinal cells but not endothelial cells of capillary. When we focus on endothelial cell of retinal capillary, endothelial expression of Jag1 in retinal capillaries is stronger in hyperglycemic mice than in normoglycemic mice. b) Quantification of endothelial Jag1 immunostaining fluorescence intensity in the retinal capillaries of the three layers (n = 6 for each group). Jag1 was markedly overexpressed in the retinal capillaries of hyperglycemic mice.

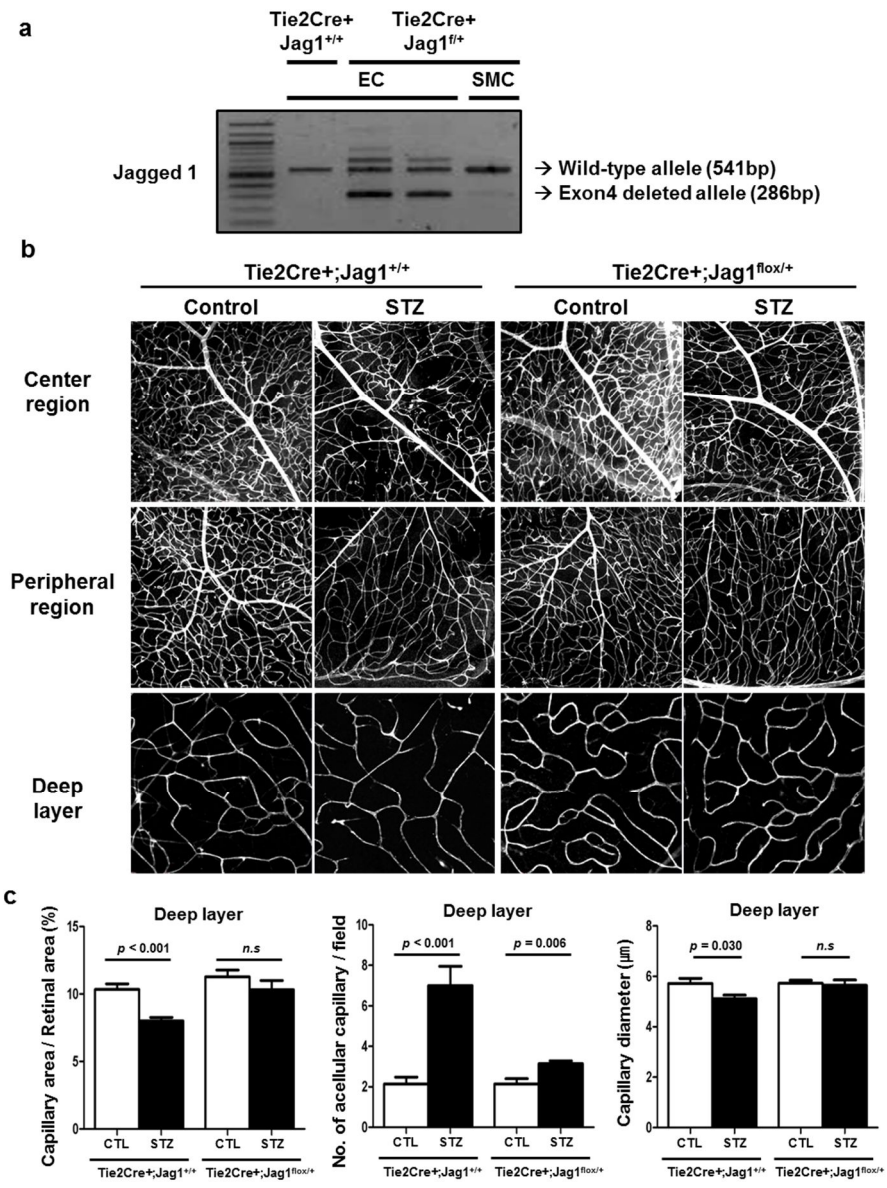

Figure 2-3. Knockdown of *Jag1* prevented retinal microvasculopathy in diabetic mice.

a) RT-PCR confirmation of EC-specific recombination induced by *Tie2-Cre* in primary aortic ECs and SMCs. The upper band (541 bp) and the lower band (286 bp) depict wild-type alleles

and *Jag1* mutant alleles lacking exon 4, respectively. The *Jag1* mutant allele was not detected in SMCs. b) BS-1 lectin staining of retinas from EC-specific *Jag1* heterozygous deficient mice (*Tie2-Cre*+;*Jag1*$^{flox/+}$) and their wild-type litter-mates (*Tie2-Cre*+;*Jag1*$^{+/+}$). Representative images of the deep layer of the retinas showed that hyperglycemia caused vasculopathy, which was prevented by knockdown of endothelial *Jag1* in diabetic mice. c) Quantification of the deep capillary layers: capillary density (n = 7 for each group), number of acellular capillaries (n = 7 for each group), and capillary diameter (n = 9 for each group).

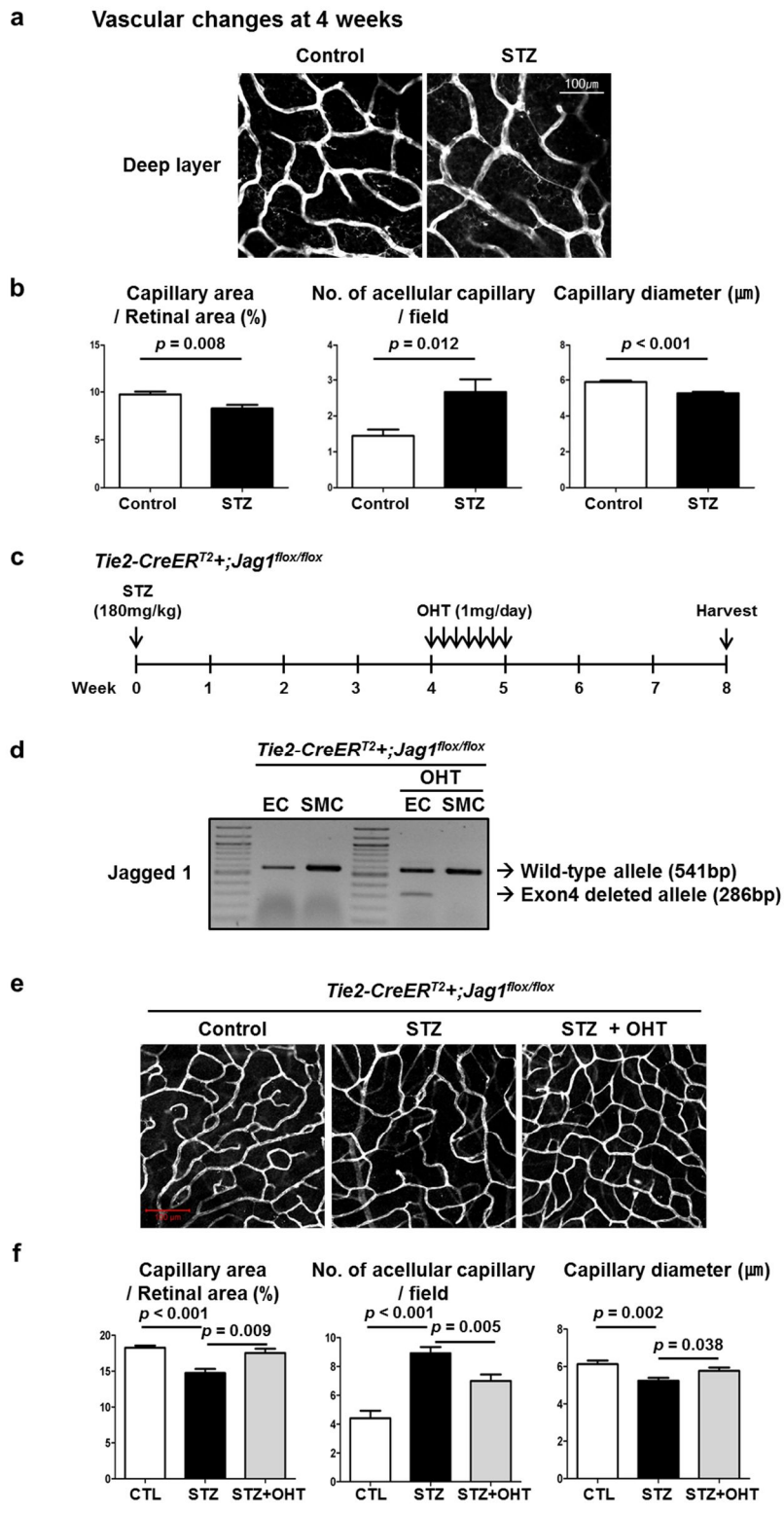
a
Vascular changes at 4 weeks
Control
STZ
100μm
Deep layer
b
Capillary area / Retinal area (%)
p = 0.008
No. of acellular capillary / field
p = 0.012
Capillary diameter (μm)
p < 0.001
Control
STZ
c
Tie2-CreER^T2+;Jag1^flox/flox
STZ (180mg/kg)
OHT (1mg/day)
Harvest
Week 0 1 2 3 4 5 6 7 8
d
Tie2-CreER^T2+;Jag1^flox/flox
OHT
EC SMC EC SMC
Jagged 1
→ Wild-type allele (541bp)
→ Exon4 deleted allele (286bp)
e
Tie2-CreER^T2+;Jag1^flox/flox
Control
STZ
STZ + OHT
f
Capillary area / Retinal area (%)
p < 0.001
p = 0.009
No. of acellular capillary / field
p < 0.001
p = 0.005
Capillary diameter (μm)
p = 0.002
p = 0.038
CTL STZ STZ+OHT

Figure 2-4. Hyperglycemic retinal vasculopathy can be reversed by *Jag1* knockdown in endothelial cells.

a) Whole-mounted retinas with lectin staining of hyperglycemic C57BL/6 mice showed that retinal vascular changes in the deep capillary layers were established as early as 4 weeks after STZ treatment. **b)** Quantification of the retinal deep layer capillaries at 4 weeks after STZ injection (n = 4 for each group). **c)** Schematic diagram of the experimental procedure. At four weeks after STZ administration, *Tie2-CreER*^{T2}+;*Jag1*$^{flox/flox}$ mice underwent intraperitoneal injection of 1 mg OHT per day for 7 consecutive days to reduce endothelial Jag1 expression *in vivo*. **d)** RT-PCR confirmation of EC-specific *Jag1* deletion induced by *Tie2-CreER*^{T2} after administration of OHT in primary aortic ECs compared with SMCs. The upper band (541 bp) and the lower band (286 bp) depict the wild-type allele and *Jag1* mutant allele lacking exon 4, respectively. **e)** BS-1 lectin stained retinas from *Tie2-CreER*^{T2}+;*Jag1*$^{flox/flox}$ mice. EC-specific knockdown of *Jag1* recovered capillary density and corrected retinal vasculopathyin in diabetic mice. **f)** Quantification of the deep retinal capillary layers: capillary density (n = 5 for each group), acellular capillaries (n = 12 for each group), and capillary diameter (n = 9 for each group).

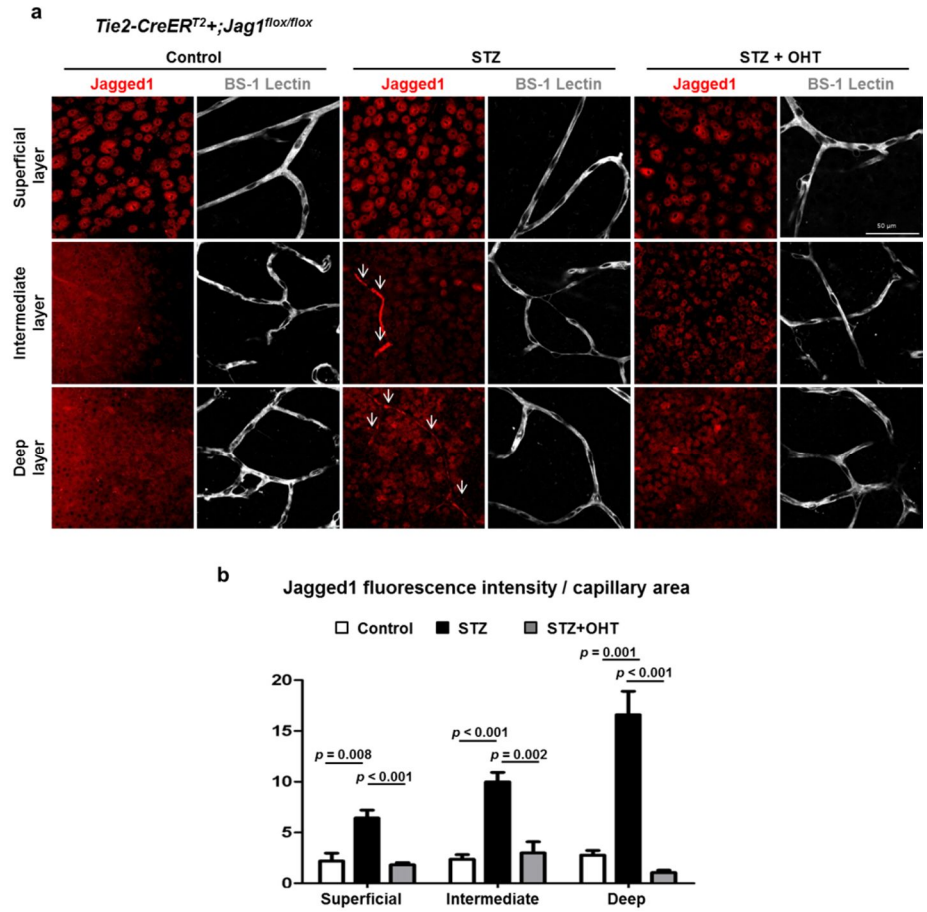

Figure 2-5. Induced knockdown of Jag1 in endothelial cells.

a) Whole-mount retinal immunofluorescence staining for Jag1 (red) and BS-1 lectin (white). *Tie2-CreER^{T2}+;Jag1$^{flox/flox}$* hyperglycemic mice without OHT showed overexpression of Jag1 in the capillaries compared to the control. Cre-mediated EC-specific Jag1 ablation was demonstrated by the absence of Jag1 staining in the *Tie2-CreER^{T2}+;Jag1$^{flox/flox}$* hyperglycemic mice receiving OHT. Arrows show Jag1 staining in the capillaries. b) Quantification of Jag1 immunostaining fluorescence intensity in retinal capillaries: control (n = 4),

STZ (n = 4), and STZ+OHT (n = 6). A marked reduction of Jag1 expression was observed in the *Tie2-CreER*^{T2}+;*Jag1*$^{flox/flox}$ hyperglycemic mice receiving OHT.

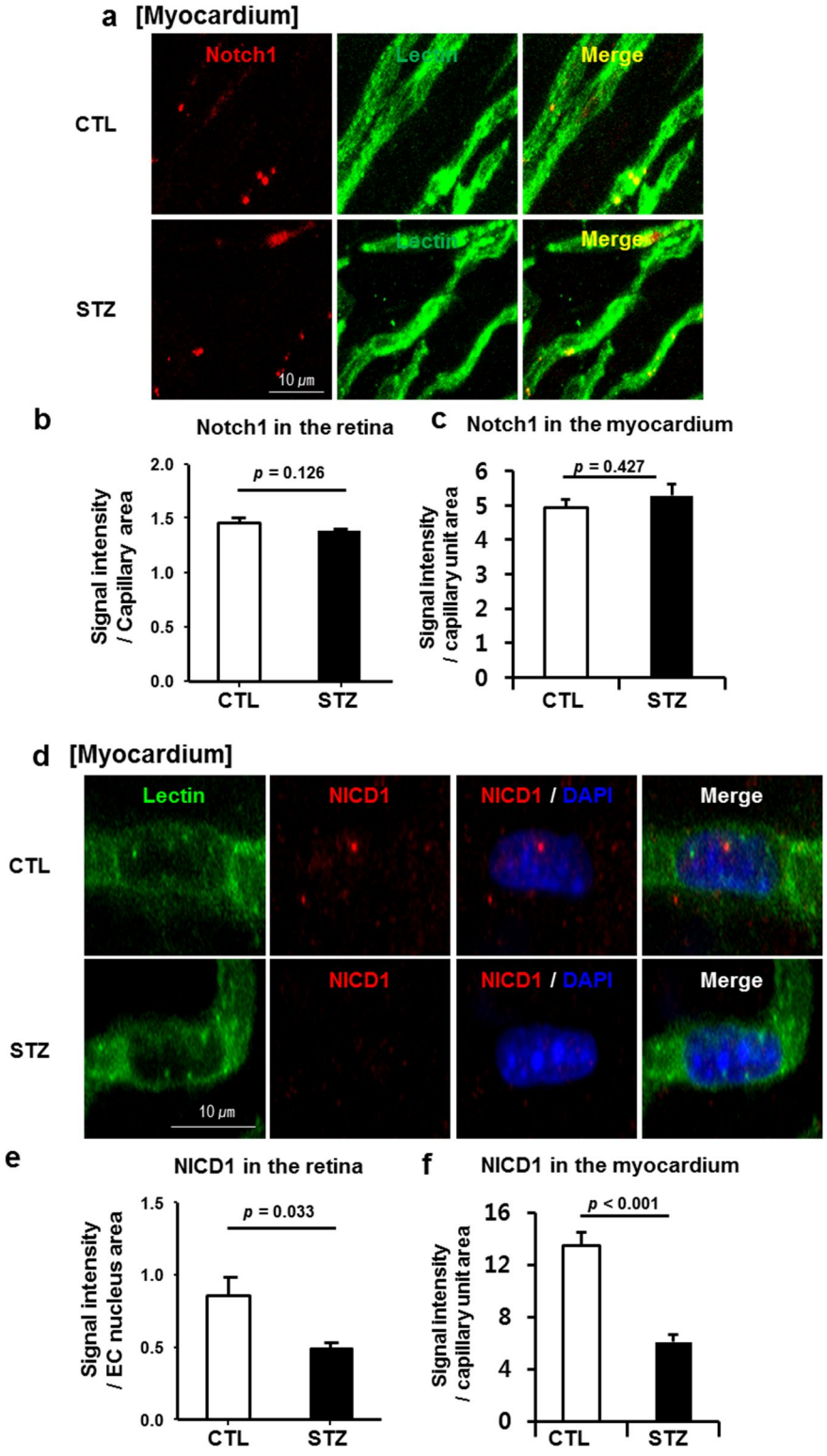
a [Myocardium]
Notch1
Lectin
Merge
CTL
STZ
10 μm
b
Notch1 in the retina
p = 0.126
Signal intensity / Capillary area
2.0
1.5
1.0
0.5
0.0
CTL
STZ
c
Notch1 in the myocardium
p = 0.427
Signal intensity / capillary unit area
6
5
4
3
2
1
0
CTL
STZ
d [Myocardium]
Lectin
NICD1
NICD1 / DAPI
Merge
CTL
STZ
10 μm
e
NICD1 in the retina
p = 0.033
Signal intensity / EC nucleus area
1.5
1.0
0.5
0.0
CTL
STZ
f
NICD1 in the myocardium
p < 0.001
Signal intensity / capillary unit area
16
12
8
4
0
CTL
STZ

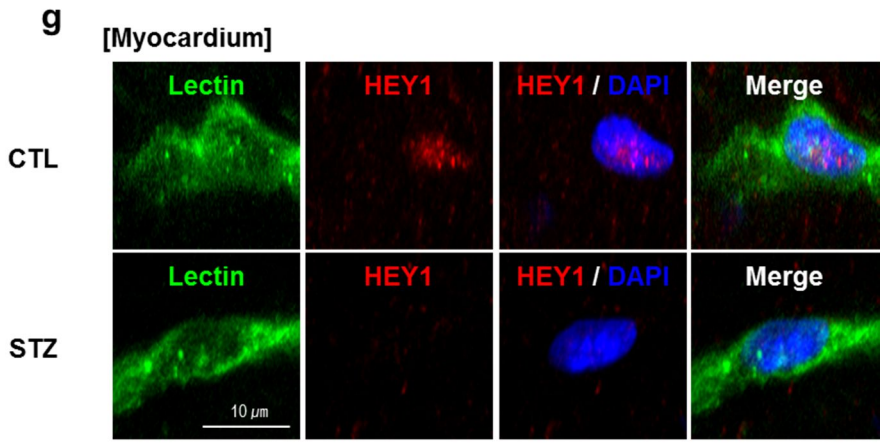
g
[Myocardium]
Lectin
HEY1
HEY1 / DAPI
Merge
CTL
STZ
10 μm

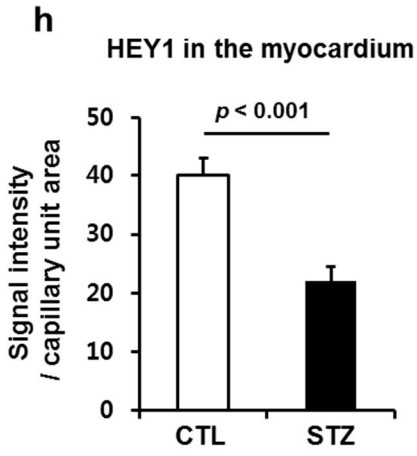
h
HEY1 in the myocardium
p < 0.001
Signal intensity
/ capillary unit area
50
40
30
20
10
0
CTL
STZ

[Myocardium]

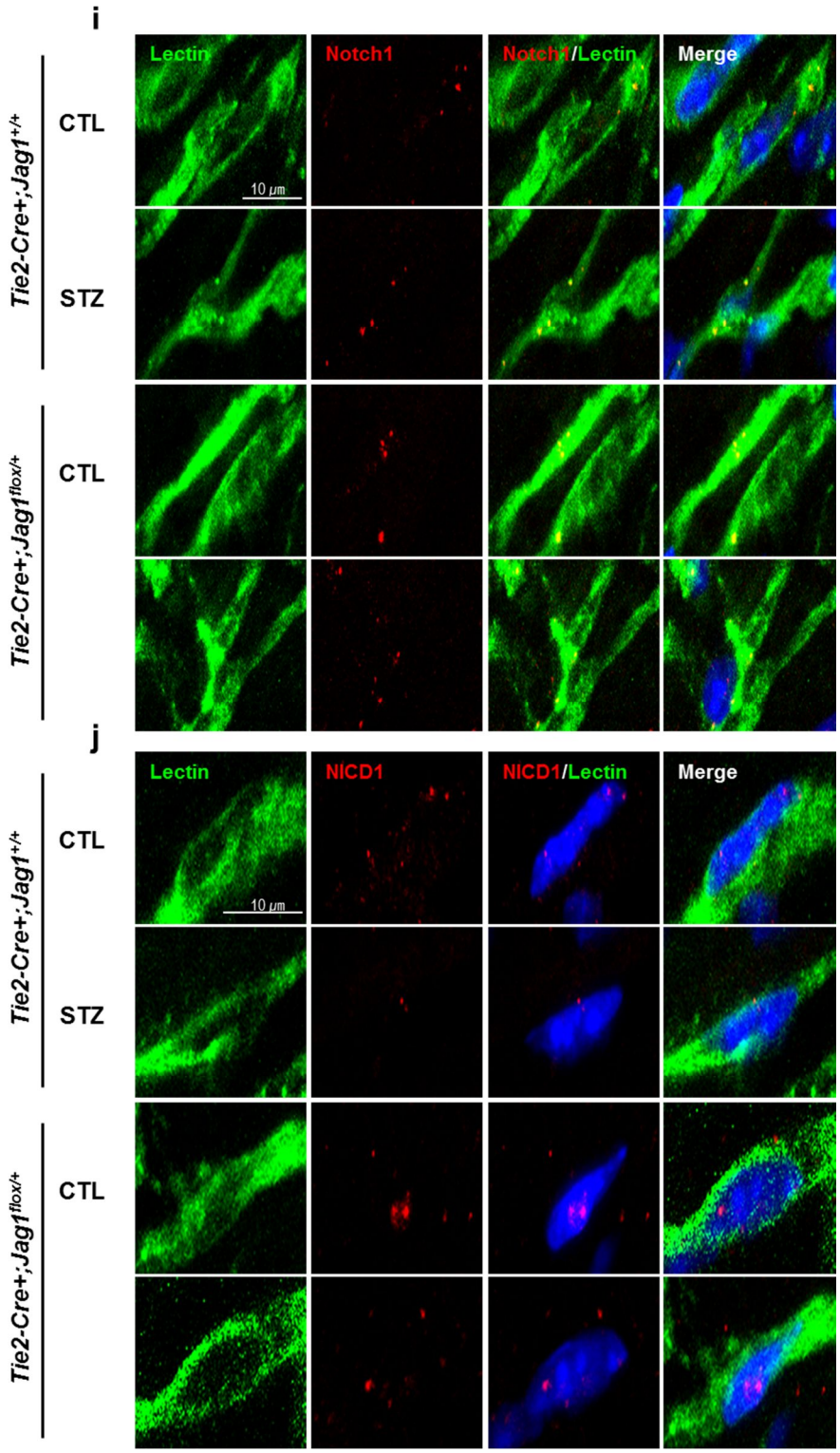
i
Lectin
Notch1
Notch1/Lectin
Merge
10 μm
Tie2-Cre+;Jag1+/+
CTL
STZ
Tie2-Cre+;Jag1flox/+
CTL
j
Lectin
NICD1
NICD1/Lectin
Merge
10 μm
Tie2-Cre+;Jag1+/+
CTL
STZ
Tie2-Cre+;Jag1flox/+
CTL

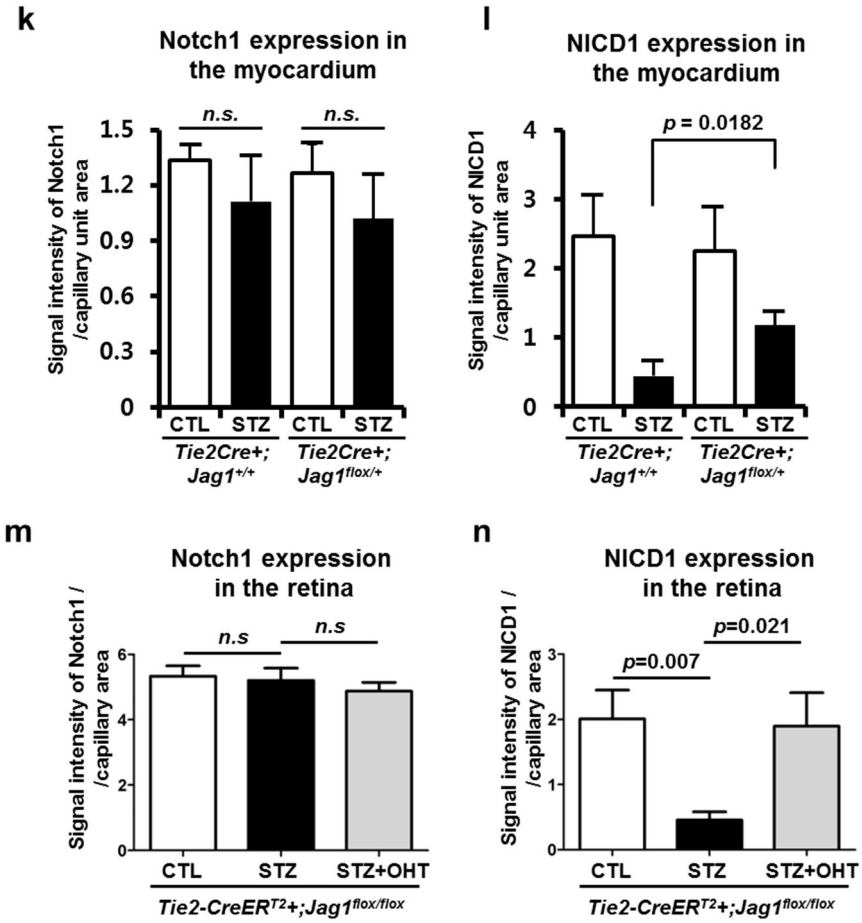

Figure 2-6. Hyperglycemia decreased Notch signal activity, which was prevented by Jag1 knockdown, in endothelial cells of myocardium as well as retina.

a) Immunofluorescence staining for Notch1 (red), and BS-1 lectin (green), in heart myocardial capillaries of control and STZ mice. b-c) Quantification of Notch1 immunostaining fluorescence intensity in retinal and heart capillaries of wild type mice displayed no difference between the normoglycemic and hyperglycemic mice (n = 7 for each group of retina, n = 3

for each group of heart. **d)** Immunofluorescence staining for NICD1 (red) in the nucleus (blue) of heart myocardial capillaries. **e–f)** NICD1 immunostaining fluorescence intensity in retinal and heart endothelial nuclei markedly decreased in the hyperglycemic mice compared to the normoglycemic control mice (n = 5 for each group's retina, n = 3 for each group's heart). **g)** Immunofluorescence staining for HEY1 (red) in the nucleus (blue) of heart myocardial capillaries. **h)** Quantification of HEY1 staining fluorescence intensity within endothelial nucleus demonstrating the decreased HEY1 expression in the nucleus of the STZ mice compared to control mice (n=3). **i–l)** Analysis of myocardial capillary showing that endothelial specific knockdown of *Jag1* recovered nuclear localization of NICD1 which was decreased by STZ. i, j) Endothelial-specific knockdown of *Jag1* using *Tie2-Cre*+;*Jag1*$^{flox/+}$ mice and control experiments using *Tie2-Cre*+;*Jag1*$^{+/+}$ mice. BS-1 lectin (green) and DAPI (blue). Notch1 (red) in i), NICD1 (red) in j). CTL: normoglycemic mice, STZ: hyperglycemic mice. **k)** Quantification of Notch1 expression (n = 2 CTL, n=3 STZ). **l)** Quantification of NICD expression (n = 3, respectively). m–n) Analysis of retinal capillaries in *Tie2-CreER*^{T2}+;*Jag1*$^{flox/flox}$ mice. **m)** Quantification of Notch1 expression (n = 3, respectively). **n)** Quantification of NICD expression (n = 3, respectively).

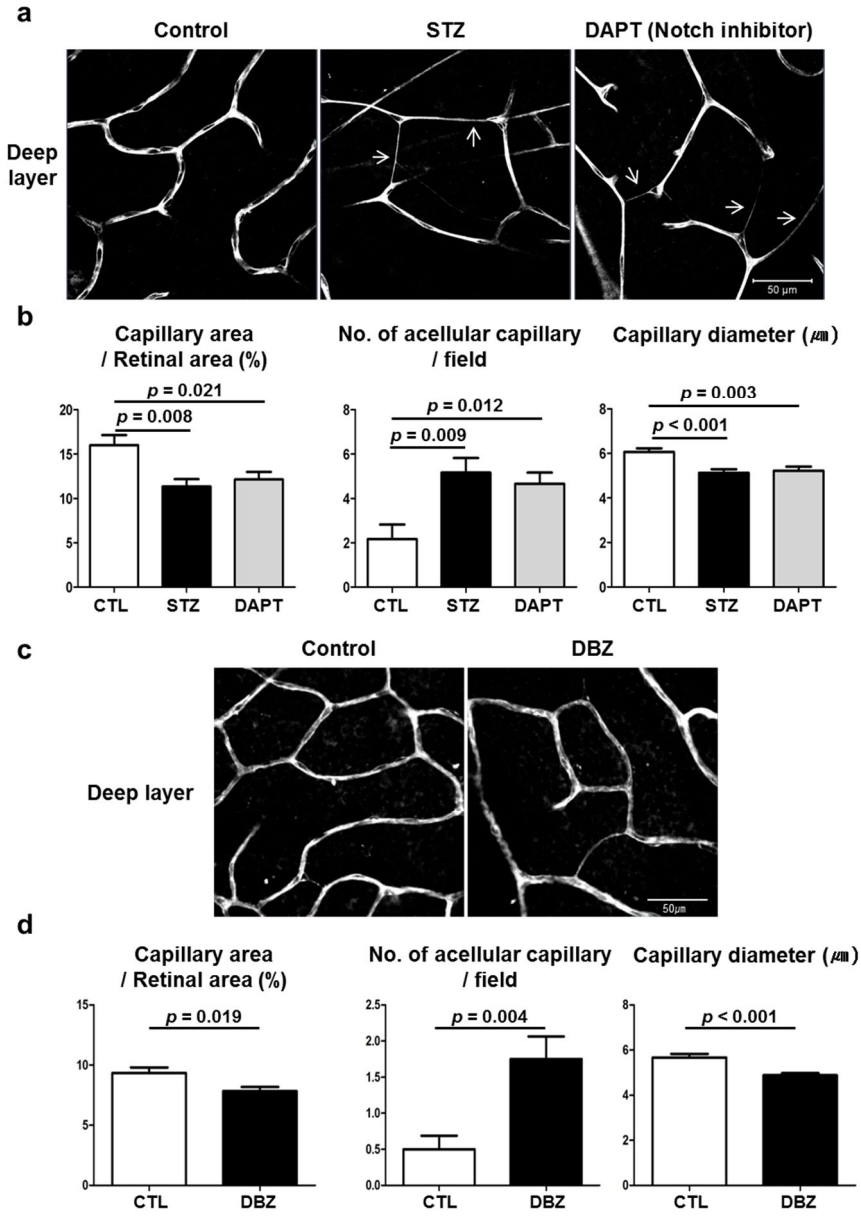

Figure 2-7. Chemical inhibition of Notch signaling phenocopied hyperglycemia-induced capillary abnormality.

a) BS-1 lectin staining of whole-mounted retinas from control, STZ-injected, and DAPT-injected mice. The retinal capillaries

of hyperglycemic mice looked very similar to that of Notch-inhibited mice (arrows: acellular capillaries). b) Quantification of vascular parameters in the deep retina layers: capillary density (n = 6 for each group), acellular capillaries (n = 6 for each group), and capillary diameter (n = 9 for each group).

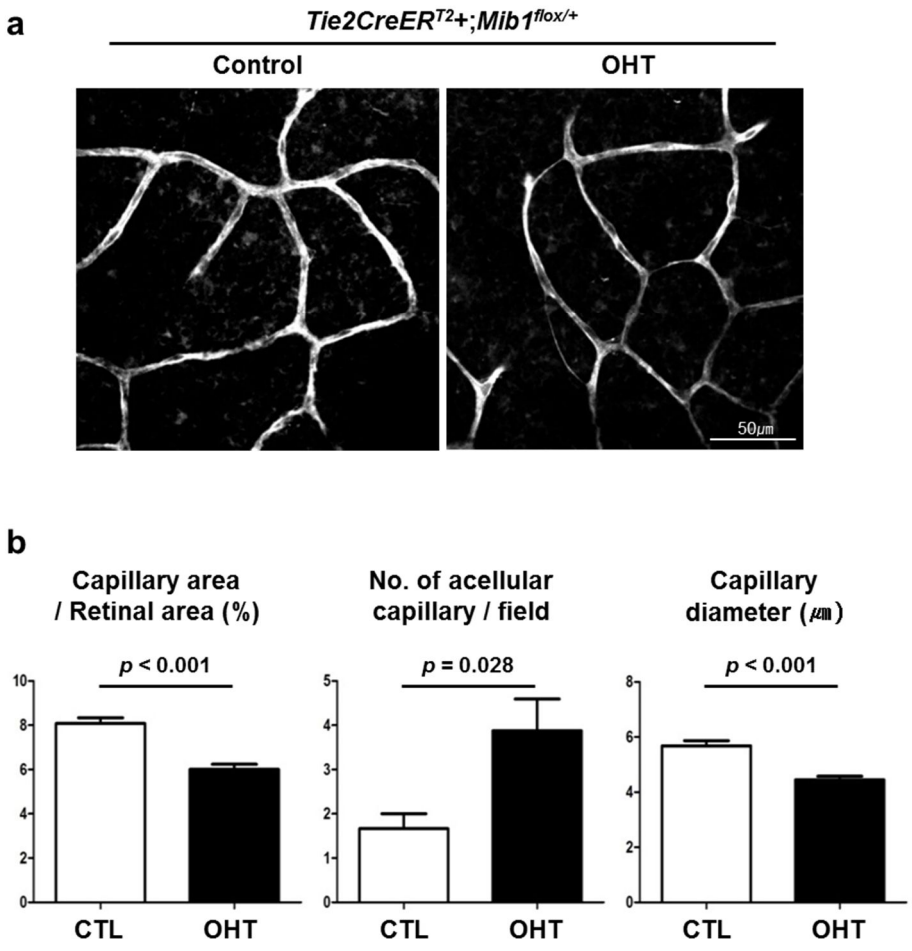
a
Tie2CreER^{T2}+;Mib1$^{flox/+}$
Control
OHT
50μm
b
Capillary area / Retinal area (%)
p < 0.001
CTL
OHT
No. of acellular capillary / field
p = 0.028
CTL
OHT
Capillary diameter (μm)
p < 0.001
CTL
OHT

c

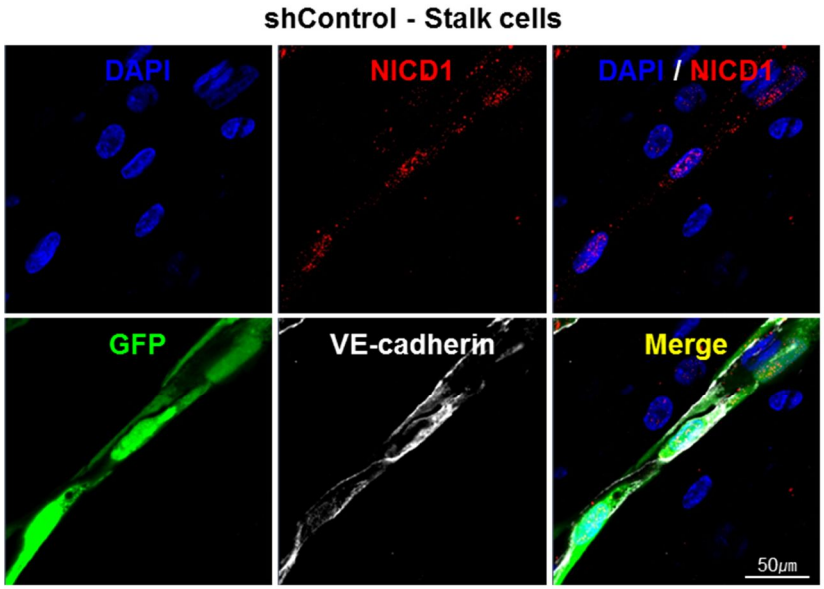
shControl - Stalk cells
DAPI
NICD1
DAPI / NICD1
GFP
VE-cadherin
Merge
50μm

d

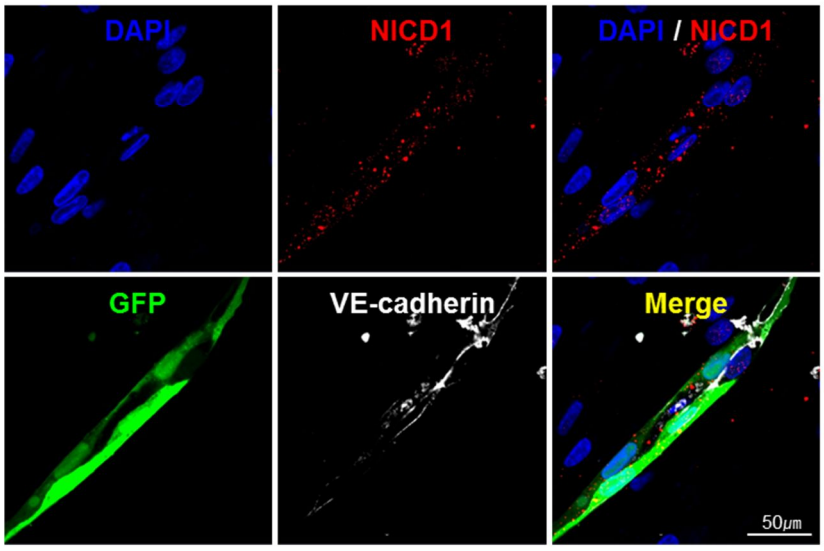
shMib-1 - Stalk cells
DAPI
NICD1
DAPI / NICD1
GFP
VE-cadherin
Merge
50μm

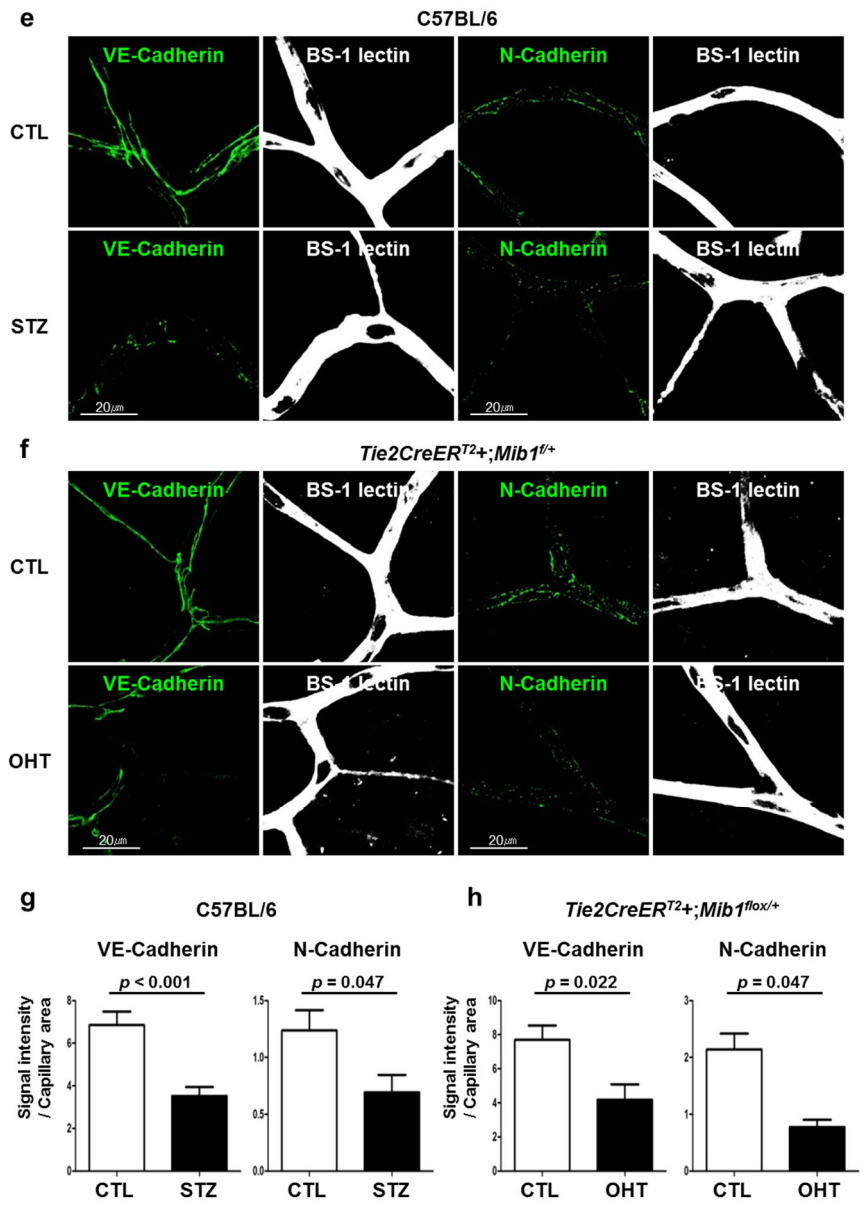

Figure 2-8. Additional genetic model confirmed that inhibition of Notch signaling recapitulated hyperglycemia-induced capillary abnormality.

a) BS-1 lectin stained whole-mounted retinas from *Tie2-CreER*^{T2}+;*Mib1*$^{flox/+}$ mice. EC-specific *Mib1* deletion by OHT administration induced retinal capillary alterations similar to those observed in hyperglycemic conditions. **b)** Quantification of the capillary changes observed in the retinal deep layers of *Tie2-CreER*^{T2}+;*Mib1*$^{flox/+}$ mice (n = 4 for each group). **c-d)** Inhibition of Notch signalingsignaling in an *in vitro* model of angiogenesis. Lentiviral shMib-1 transduction in ECs reduced NICD nuclear localization and VE-cadherin expression. **e-f)** Representative capillary-cropped immunofluorescence staining images of whole-mount retinas. Reduced expressions of VE-cadherin and N-cadherin were observed in both STZ-induced hyperglycemic C57BL/6 mice (e) and Notch-inhibited mice using *Tie2-CreER*^{T2}+;*Mib1*$^{flox/+}$ mice with OHT treatment (inducible Mib downregulation) (f). **g)** Quantifications of endothelial VE-cadherin immunofluorescence (n = 6 for each group of C57BL/6 mice) **h)** Quantifications of endothelial N-cadherin immunofluorescence (n = 5 for each group of *Tie2-CreER*^{T2}+;*Mib1*$^{flox/+}$ mice)

DISCUSSION

We show that hyperglycemia induces RM, characterized by capillary remodeling, regression, or decreased density in adult mice. Notch ligand Jag1, but not Dll4, was markedly increased in the ECs of hyperglycemic mice. When Jag1 expression was attenuated, as in endothelial specific−*Jag1* knockdown mice, RM was effectively prevented, even under hyperglycemic conditions. Furthermore, when endothelial Jag1 expression was suppressed 4 weeks after the hyperglycemia induction in inducible endothelial Jag1 knockdown mice, RM was reversed and the retinal vasculature was normalized, suggesting therapeutic potential at this target. Hyperglycemia and Jag1 overexpression decreased the nuclear localization of NICD1 in ECs. Chemical Notch inhibition phenocopied RM in normal mice. Hyperglycemia and Notch inhibition decreased endothelial junctional molecules, which led to capillary regression.

Intercellular signaling as a novel mechanism of diabetic microvasculopathy

ECs and pericytes are implicated in the progression toward classic diabetic microvascular disease. Molecular mechanisms included the induction of the aldose reductase pathway, protein kinase C, oxidative stress, protein glycation, or hexosamine pathway[40]. These intracellular changes are suggested to cause apoptosis of endothelial cells and pericytes as well as leukocyte trafficking resulting in microvasculopathy[41]. However, we did not find a significant increase in endothelial apoptosis in the hyperglycemic retina by all apoptosis detection methods including TUNEL staining, cleaved caspase 3 staining, PI, and annexin V although there was RM in the present study. These facts warrant investigation of another mechanism for early microvasculopathy.

Recently, intercellular signaling between adjacent ECs has been reported to play important roles in development, remodeling, and homeostasis of vessels[2]. Delicate regulation and balance between tip cells and stalk cells via cell-to-cell signaling are needed in vascular biology. Therefore, we investigated the role of intercellular signaling in adult capillaries under the diabetic condition. Since ECs in the capillaries dynamically change by intercellular signaling[8], we predicted that we would be able to

observe changes of intercellular signaling in the capillaries after exposure to hyperglycemia. As a result, we could identify the disturbed Jag1/Notch signaling in capillaries of our diabetic mouse model.

Disturbed Jag1 and Notch signaling in a murine hyperglycemic model

Notch signaling is closely related to the formation and maintenance of the vascular system[1, 5, 6]. Notch1 and its ligands, Dll4 and Jag1, are well-known molecules involved in intercellular signaling in the vessels.

The most prominent change in the ECs of hyperglycemic mice was the induction of Jag1 in the present study. It is interesting that Dll4, another ligand for Notch, did not changed in the diabetic condition, suggesting the specific response of Jag1 to hyperglycemia. We previously reported the in vitro observation that hyperglycemia increased endothelial expression of Jag1 through NF-κB and PKC[42], which was corroborated by other reports that PKC induces NF-κB2, the upstream regulator of Jag1[30]. We tested the causal relationship between Jag1 induction and RM in hyperglycemia using two different

genetically engineered mouse models: (1) mice with endothelium-specific knockdown of *Jag1* and (2) mice with endothelium-specific 'inducible' knockdown of *Jag1*. In the first model, we confirmed that blocking Jag1 could prevent the development of RM even in the diabetic condition. In the second model, we observed the valuable result that modulation of Jag1 may be a therapeutic strategy for established RM in diabetic condition. Induction of *Jag1* knockdown in ECs at 4 weeks after hyperglycemia or the establishment of RM could reverse RM, resulting in the normalization of retinal vasculature in hyperglycemia. Because not only the retina but also the heart, limb muscle, kidney, and in vitro human endothelial cells (HUVEC) showed Jag1 overexpression in response to hyperglycemia, Jag1 overexpression seems to be a generalized endothelial response to hyperglycemia.

As a downstream mechanism after induction of Jag1 in hyperglycemic ECs, we evaluated the Notch signaling by assessment of total Notch1 and NICD1. Endothelial Notch signaling is crucial for the remodeling of veins and the perivenous capillary plexus in the postnatal retina[39]. In the present study, we found that nuclear localization of NICD1 was

suppressed in the retinal ECs of diabetic mice, whereas total Notch1 was not affected. Jag1 can inhibit Notch signaling as a cell autonomous process, known as cis-inhibition[33]. In the signal-receiving cells, the overexpressed Jag1 may bind and inhibit Notch in the same cells (cis-inhibition), which inhibits trans-activation from the signal-sending cells (like Dll4 on adjacent cells). The balance between Dll4 and Jag1 is important in regulating Notch signaling and vascular growth[43]. In the present study we found that hyperglycemia induced an imbalance between Jag1 and Dll4, favoring Jag1 and resulting in the suppression of nuclear localization of NICD1 Notch activity. Our findings that chemical and genetic Notch inhibition phenocopied RM demonstrates the importance of Notch suppression in the pathobiology of RM under diabetic conditions. We previously reported a high glucose-induced abnormal angiogenesis in an in vitro model using human endothelial cells, which included increased numbers of regressing tubes, and decreased vascular diameter, length, area, and growing tubes[42]. We suggest that Jag1 overexpression and inhibition of Notch1 signaling are the underlying mechanism of the abnormalities.

The disturbed Jag1/Notch signaling may be the key mechanism of RM in diabetes.

Interestingly, endothelial glucose metabolism is reported to affect Notch signaling and developmental angiogenesis[38]. De Bock and colleagues have shown that increased endothelial glucose metabolism by overexpression of phosphofructokinase-2/fructose-2,6-bisphosphatase, a glycolytic enzyme in ECs, masked the vascular stabilizing activity of Notch, whereas decreased glycolysis in ECs impaired tip cell formation upon Notch blockade, implying that glycolysis in endothelial cells regulates vessel branching[38]. Intriguingly, Notch signaling disturbance in the upregulated glycolysis was similar to that in the hyperglycemic condition in our study. In that condition, ECs take up a high level of glucose into their cytoplasm, which may mimic the condition with overexpressed glycolytic enzyme.

A different vascular response between the postnatal and the adult mice after endothelial notch inhibition

The most interesting finding in the present study is that capillary rarefaction after notch inhibition in adult mice occurs

in contrast to the hypersprouting and increased angiogenesis in postnatal angiogenesis. We observed a number of different occurrences in the adult retina. First, the expression of VEGFR2 and VEGFR3 in the adult retina was weak compared to that in the postnatal retina, and not changed after hyperglycemia. VEGF receptor downregulation during vascular maturation was reported in a previous study[39]. Second, endothelial proliferation is very rare and not increased in the adult retina. This is also consistent with the previous report[39]. VEGF signaling and endothelial proliferation are necessary for postnatal sprouting angiogenesis. The lack of angiogenic signaling might be the reason why Notch inhibition does not induce sprouting angiogenesis in the adult retina.

Third, endothelial junctional Notch is known to regulate the transcription of N-cadherin through associating with the Notch intracellular complex at the RBP-J binding site of the N-cadherin promoter[44]. Notch activity is also quantitatively related with VE-cadherin turnover and mobility at endothelial cell junctions during angiogenic sprouting[45]. We found that VE-cadherin and N-cadherin were significantly reduced in the hyperglycemic mice and the mice with lower Notch activity.

These findings reveal that a decrease of endothelial Notch signaling in the adult results in microvascular abnormalities without angiogenesis. Fourth, in contrast to the many ECs found within postnatal capillaries, matured capillaries in the retina contained tubules formed by single, hollowed ECs, single ECs with autocellular junctions, or two ECs with two adherens junctions[39]. We found that hyperglycemia or Notch inhibition increased single, hollowed ECs and an autocellular junction with loss of lumens. The different capillary composition may also be related to capillary rarefaction after Notch inhibition in the adult.

A novel target to control diabetic microvasculopathy other than glucose control

It is well known that diabetic microvasculopathy can be prevented by intensive glucose control[10, 35]. However, intensive this is almost always associated with serious complications like hypoglycemia[36]. Until now, therapeutic trials by targeting the previously proposed pathophysiology of diabetic vasculopathy have failed to prove clinical efficacy because, in part, the mechanism of diabetic vasculopathy is too complex and

heterogeneous for one to decide on a target[14]. However, intercellular signaling has not been tested as a target.

We found that the capillary was a dynamic structure undergoing sprouting and regression, which is regulated by Notch signaling. Thus, we surmise that capillary integrity and Notch signaling should be further evaluated in various vascular diseases, including hypertension, diabetes mellitus, and microvascular angina. Specifically, we revealed, for the first time, that Notch signaling in adult mice was affected by hyperglycemia, a potentially novel mechanism of diabetic microvasculopathy at an early phase. Until now, the only treatment to prevent diabetic microvasculopathy has been intensive glucose control, which may cause fatal hypoglycemia[35]. Therefore, novel molecular targets are required. In this context, Jag1 or Notch signaling in ECs may be feasible therapeutic targets for diabetic microvasculopathy. In this study, a chemical inhibitor of Notch signaling easily phenocopied hyperglycemia-induced RM, suggesting the possibility of a chemical agonist of Notch signaling as a new option to prevent diabetic RM. Furthermore, using endothelium-specific 'inducible' knockdown mice, we showed that downregulation of *Jag1* after establishment of RM

in hyperglycemia could reverse RM and normalize the retinal vasculature even in a hyperglycemic condition. This finding may be the basis for the development of new therapeutic strategies to treat diabetic RM.

Limitations

It is not possible to assess all forms of cell death in vivo. Particularly, necrosis, necroptosis, and late apoptosis cannot be distinguished by single observation with conventional staining methods. Therefore, we could not rule out other enhanced forms of cell death in the hyperglycemic mice.

There may be some differences in the level of Jag1 expression in the retinal cells compared to other endothelial cells. Since other endothelial cells are beyond the scope of this study, we did not perform any further experiments to assess the generalizability of retinal cells. We, however, do not think that any potential difference of Jag1 expression in the retinal cells compared to other endothelial cells diminishes the importance of endothelial Notch signaling in the mechanism of diabetic microvasculopathy because endothelial-specific modulation of Jag1 did change capillaries in the hyperglycemic mice.

Taken together, our results show that hyperglycemia induces Jag1 overexpression and suppresses Notch signaling in ECs, leading to RM in adult mice. We conclude that dysregulated intercellular Notch signaling may be a novel mechanism explaining diabetic microvasculopathy (Figure 2-9).

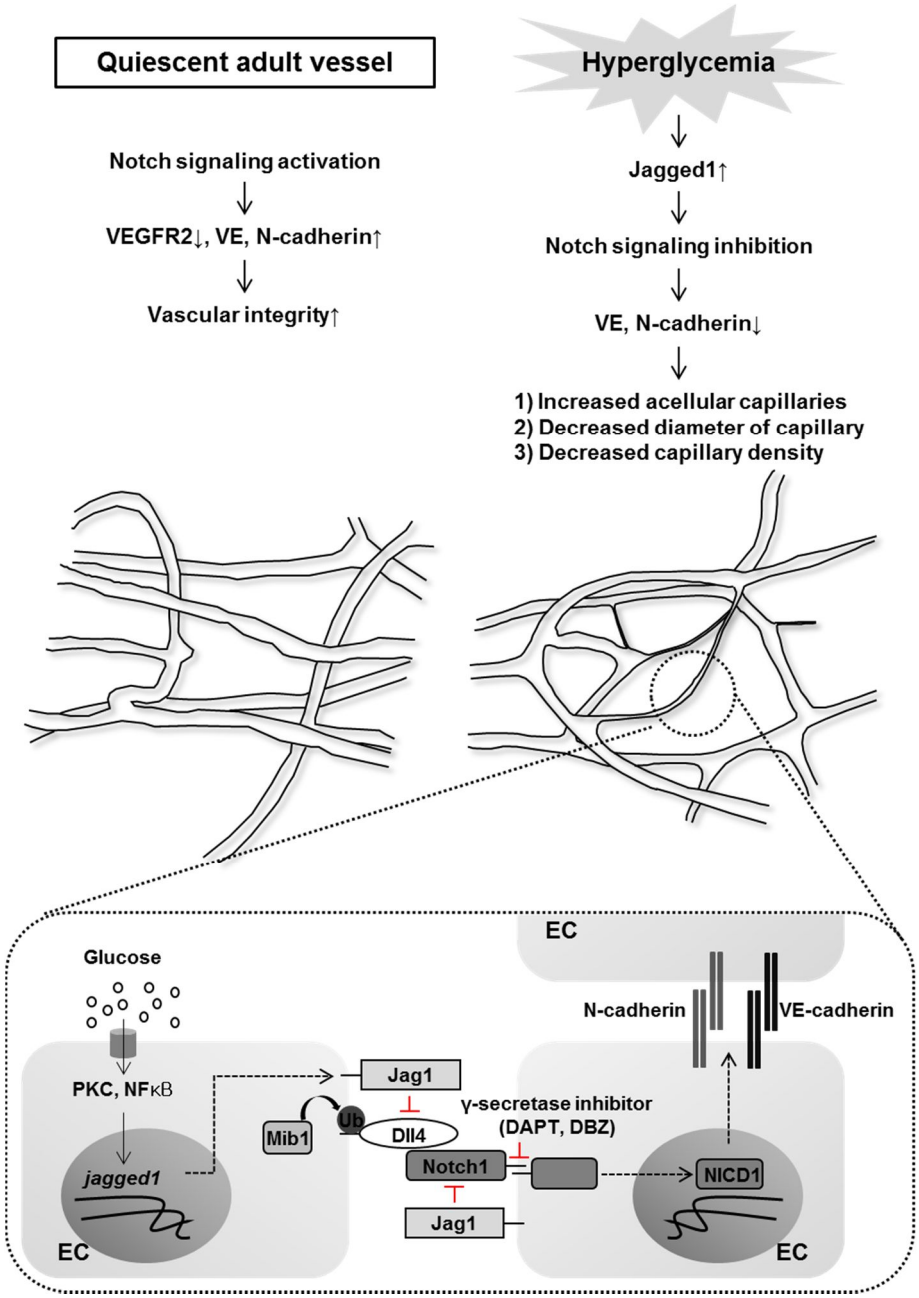

Figure 2-9. A schematic figure of the suggested mechanism of diabetic retinal microvasculopathy.

REFERENCES

1. Phng LK and Gerhardt H. Angiogenesis: a team effort coordinated by notch. *Dev Cell*. 2009;16:196-208.
2. Potente M, Gerhardt H and Carmeliet P. Basic and therapeutic aspects of angiogenesis. *Cell*. 2011;146:873-87.
3. Carmeliet P and Jain RK. Molecular mechanisms and clinical applications of angiogenesis. *Nature*. 2011;473:298-307.
4. Gerhardt H, Golding M, Fruttiger M, Ruhrberg C, Lundkvist A, Abramsson A, Jeltsch M, Mitchell C, Alitalo K, Shima D and Betsholtz C. VEGF guides angiogenic sprouting utilizing endothelial tip cell filopodia. *J Cell Biol*. 2003;161:1163-77.
5. Hellstrom M, Phng LK, Hofmann JJ, Wallgard E, Coultas L, Lindblom P, Alva J, Nilsson AK, Karlsson L, Gaiano N, Yoon K, Rossant J, Iruela-Arispe ML, Kalen M, Gerhardt H and Betsholtz C. Dll4 signalling through Notch1 regulates formation of tip cells during angiogenesis. *Nature*. 2007;445:776-80.
6. Benedito R, Roca C, Sorensen I, Adams S, Gossler A, Fruttiger M and Adams RH. The notch ligands Dll4 and Jagged1 have opposing effects on angiogenesis. *Cell*. 2009;137:1124-35.
7. Jakobsson L, Franco CA, Bentley K, Collins RT, Ponsioen B, Aspalter IM, Rosewell I, Busse M, Thurston G, Medvinsky A, Schulte-Merker S and Gerhardt H. Endothelial cells dynamically compete for the tip cell position during angiogenic sprouting. *Nat Cell Biol*. 2010;12:943-53.
8. Arima S, Nishiyama K, Ko T, Arima Y, Hakozaki Y, Sugihara K, Koseki H, Uchijima Y, Kurihara Y and Kurihara H. Angiogenic morphogenesis driven by dynamic and heterogeneous collective endothelial cell movement. *Development*. 2011;138:4763-76.
9. Takebe T, Sekine K, Enomura M, Koike H, Kimura M, Ogaeri T, Zhang RR, Ueno Y, Zheng YW, Koike N, Aoyama S, Adachi Y and Taniguchi H. Vascularized and functional human liver from an iPSC-derived organ bud transplant. *Nature*. 2013;499:481-4.
10. The effect of intensive treatment of diabetes on the development and progression of long-term complications in insulin-dependent diabetes mellitus. The Diabetes Control and Complications Trial Research Group. *N Engl J Med*. 1993;329:977-86.
11. Nathan DM, Cleary PA, Backlund JY, Genuth SM, Lachin JM, Orchard TJ, Raskin P, Zinman B, Diabetes C, Complications Trial/Epidemiology of Diabetes I and Complications Study Research G. Intensive diabetes treatment and cardiovascular disease in patients with type 1 diabetes. *N Engl J Med*. 2005;353:2643-53.
12. Group AC, Patel A, MacMahon S, Chalmers J, Neal B, Billot L, Woodward M, Marre M, Cooper M, Glasziou P, Grobbee D, Hamet P,

Harrap S, Heller S, Liu L, Mancia G, Mogensen CE, Pan C, Poulter N, Rodgers A, Williams B, Bompoint S, de Galan BE, Joshi R and Travert F. Intensive blood glucose control and vascular outcomes in patients with type 2 diabetes. *N Engl J Med*. 2008;358:2560-72.
13. Mazzone T, Chait A and Plutzky J. Cardiovascular disease risk in type 2 diabetes mellitus: insights from mechanistic studies. *Lancet*. 2008;371:1800-9.
14. Orasanu G and Plutzky J. The pathologic continuum of diabetic vascular disease. *J Am Coll Cardiol*. 2009;53:S35-42.
15. Geraldes P, Hiraoka-Yamamoto J, Matsumoto M, Clermont A, Leitges M, Marette A, Aiello LP, Kern TS and King GL. Activation of PKC-delta and SHP-1 by hyperglycemia causes vascular cell apoptosis and diabetic retinopathy. *Nat Med*. 2009;15:1298-306.
16. Lee HY, Youn SW, Oh BH and Kim HS. Kruppel-like factor 2 suppression by high glucose as a possible mechanism of diabetic vasculopathy. *Korean Circ J*. 2012;42:239-45.
17. Hoshi H and McKeehan WL. Isolation, growth requirements, cloning, prostacyclin production and life-span of human adult endothelial cells in low serum culture medium. *In Vitro Cell Dev Biol*. 1986;22:51-6.
18. Schachinger V, Erbs S, Elsasser A, Haberbosch W, Hambrecht R, Holschermann H, Yu J, Corti R, Mathey DG, Hamm CW, Suselbeck T, Assmus B, Tonn T, Dimmeler S, Zeiher AM and Investigators R-A. Intracoronary bone marrow-derived progenitor cells in acute myocardial infarction. *N Engl J Med*. 2006;355:1210-21.
19. Yoon CH, Koyanagi M, Iekushi K, Seeger F, Urbich C, Zeiher AM and Dimmeler S. Mechanism of improved cardiac function after bone marrow mononuclear cell therapy: role of cardiovascular lineage commitment. *Circulation*. 2010;121:2001-11.
20. Rubinson DA, Dillon CP, Kwiatkowski AV, Sievers C, Yang L, Kopinja J, Rooney DL, Zhang M, Ihrig MM, McManus MT, Gertler FB, Scott ML and Van Parijs L. A lentivirus-based system to functionally silence genes in primary mammalian cells, stem cells and transgenic mice by RNA interference. *Nat Genet*. 2003;33:401-6.
21. Cho HJ, Lee CS, Kwon YW, Paek JS, Lee SH, Hur J, Lee EJ, Roh TY, Chu IS, Leem SH, Kim Y, Kang HJ, Park YB and Kim HS. Induction of pluripotent stem cells from adult somatic cells by protein-based reprogramming without genetic manipulation. *Blood*. 2010;116:386-95.
22. Vailhe B, Vittet D and Feige JJ. In vitro models of vasculogenesis and angiogenesis. *Lab Invest*. 2001;81:439-52.
23. Alajati A, Laib AM, Weber H, Boos AM, Bartol A, Ikenberg K, Korff T, Zentgraf H, Obodozie C, Graeser R, Christian S, Finkenzeller G, Stark GB, Heroult M and Augustin HG. Spheroid-based engineering of a human vasculature in mice. *Nat Methods*. 2008;5:439-45.

24. Koh W, Stratman AN, Sacharidou A and Davis GE. In vitro three dimensional collagen matrix models of endothelial lumen formation during vasculogenesis and angiogenesis. *Methods Enzymol*. 2008;443:83-101.
25. Noseda M, Chang L, McLean G, Grim JE, Clurman BE, Smith LL and Karsan A. Notch activation induces endothelial cell cycle arrest and participates in contact inhibition: role of p21Cip1 repression. *Mol Cell Biol*. 2004;24:8813-22.
26. Curry CL, Reed LL, Nickoloff BJ, Miele L and Foreman KE. Notch-independent regulation of Hes-1 expression by c-Jun N-terminal kinase signaling in human endothelial cells. *Lab Invest*. 2006;86:842-52.
27. Zhang J, Fukuhara S, Sako K, Takenouchi T, Kitani H, Kume T, Koh GY and Mochizuki N. Angiopoietin-1/Tie2 signal augments basal Notch signal controlling vascular quiescence by inducing delta-like 4 expression through AKT-mediated activation of beta-catenin. *J Biol Chem*. 2011;286:8055-66.
28. Sainson RC, Johnston DA, Chu HC, Holderfield MT, Nakatsu MN, Crampton SP, Davis J, Conn E and Hughes CC. TNF primes endothelial cells for angiogenic sprouting by inducing a tip cell phenotype. *Blood*. 2008;111:4997-5007.
29. Romeo G, Liu WH, Asnaghi V, Kern TS and Lorenzi M. Activation of nuclear factor-kappaB induced by diabetes and high glucose regulates a proapoptotic program in retinal pericytes. *Diabetes*. 2002;51:2241-8.
30. Johnston DA, Dong B and Hughes CC. TNF induction of jagged-1 in endothelial cells is NFkappaB-dependent. *Gene*. 2009;435:36-44.
31. Artavanis-Tsakonas S, Rand MD and Lake RJ. Notch signaling: cell fate control and signal integration in development. *Science*. 1999;284:770-6.
32. De Smet F, Segura I, De Bock K, Hohensinner PJ and Carmeliet P. Mechanisms of vessel branching: filopodia on endothelial tip cells lead the way. *Arterioscler Thromb Vasc Biol*. 2009;29:639-49.
33. Fiuza UM, Klein T, Martinez Arias A and Hayward P. Mechanisms of ligand-mediated inhibition in Notch signaling activity in Drosophila. *Dev Dyn*. 2010;239:798-805.
34. Yang LT, Nichols JT, Yao C, Manilay JO, Robey EA and Weinmaster G. Fringe glycosyltransferases differentially modulate Notch1 proteolysis induced by Delta1 and Jagged1. *Mol Biol Cell*. 2005;16:927-42.
35. Intensive blood-glucose control with sulphonylureas or insulin compared with conventional treatment and risk of complications in patients with type 2 diabetes (UKPDS 33). UK Prospective Diabetes Study (UKPDS) Group. *Lancet*. 1998;352:837-53.

36. Dluhy RG and McMahon GT. Intensive glycemic control in the ACCORD and ADVANCE trials. *N Engl J Med*. 2008;358:2630-3.
37. Stratton IM, Adler AI, Neil HA, Matthews DR, Manley SE, Cull CA, Hadden D, Turner RC and Holman RR. Association of glycaemia with macrovascular and microvascular complications of type 2 diabetes (UKPDS 35): prospective observational study. *BMJ*. 2000;321:405-12.
38. De Bock K, Georgiadou M, Schoors S, Kuchnio A, Wong BW, Cantelmo AR, Quaegebeur A, Ghesquiere B, Cauwenberghs S, Eelen G, Phng LK, Betz I, Tembuyser B, Brepoels K, Welti J, Geudens I, Segura I, Cruys B, Bifari F, Decimo I, Blanco R, Wyns S, Vangindertael J, Rocha S, Collins RT, Munck S, Daelemans D, Imamura H, Devlieger R, Rider M, Van Veldhoven PP, Schuit F, Bartrons R, Hofkens J, Fraisl P, Telang S, Deberardinis RJ, Schoonjans L, Vinckier S, Chesney J, Gerhardt H, Dewerchin M and Carmeliet P. Role of PFKFB3-driven glycolysis in vessel sprouting. *Cell*. 2013;154:651-63.
39. Ehling M, Adams S, Benedito R and Adams RH. Notch controls retinal blood vessel maturation and quiescence. *Development*. 2013;140:3051-61.
40. Sheetz MJ and King GL. Molecular understanding of hyperglycemia's adverse effects for diabetic complications. *JAMA*. 2002;288:2579-88.
41. Arita R, Hata Y, Nakao S, Kita T, Miura M, Kawahara S, Zandi S, Almulki L, Tayyari F, Shimokawa H, Hafezi-Moghadam A and Ishibashi T. Rho kinase inhibition by fasudil ameliorates diabetes-induced microvascular damage. *Diabetes*. 2009;58:215-26.
42. Yoon CH, Choi YE, Koh SJ, Choi JI, Park YB and Kim HS. High glucose-induced jagged 1 in endothelial cells disturbs notch signaling for angiogenesis: a novel mechanism of diabetic vasculopathy. *J Mol Cell Cardiol*. 2014;69:52-66.
43. Bentley K, Mariggi G, Gerhardt H and Bates PA. Tipping the balance: robustness of tip cell selection, migration and fusion in angiogenesis. *PLoS Comput Biol*. 2009;5:e1000549.
44. Li F, Lan Y, Wang Y, Wang J, Yang G, Meng F, Han H, Meng A, Wang Y and Yang X. Endothelial Smad4 maintains cerebrovascular integrity by activating N-cadherin through cooperation with Notch. *Dev Cell*. 2011;20:291-302.
45. Bentley K, Franco CA, Philippides A, Blanco R, Dierkes M, Gebala V, Stanchi F, Jones M, Aspalter IM, Cagna G, Westrom S, Claesson-Welsh L, Vestweber D and Gerhardt H. The role of differential VE-cadherin dynamics in cell rearrangement during angiogenesis. *Nat Cell Biol*. 2014;16:309-21.

국문 초록

당뇨병 환자는 신장, 심장, 망막, 하지 등 신체 주요 장기에 발생하는 혈관 합병증으로 만성콩팥병, 협심증, 심근경색증, 실명, 하지허혈증 등의 발병률이 높다. 당뇨병 환자의 혈관합병증은 치료도 어렵고 치료하여도 재발이 잦아 결과가 좋지 않은 특징이 있지만, 아쉽게도 당뇨병 환자의 혈관병을 예방하고 치료하는 데에는 혈당 조절 외에 뾰족한 방법이 없다. 그 이유는 아직도 당뇨병 환자의 혈관병이 왜 발생하고 악화되는지에 대해서 잘 모르기 때문이다.

지금까지의 연구 경향은 당뇨병이 개별 혈관세포 내에서 일으키는 변화에만 집중하여, 개별 혈관세포의 사멸이 당뇨 혈관병의 주된 원인이라고 보고 있다. 하지만 본 연구에서는 당뇨병이 있는 쥐에서 혈관합병증이 발생하지만 혈관세포에서 세포 사멸은 두드러지지 않은 현상에 주목하고, 개별혈관세포의 문제보다는 혈관세포들 사이의 신호전달체계가 교란되어 혈관의 안정상태가 무너지는 것에서 혈관합병증의 새로운 발생 원인을 찾고자 하였다.

본 연구에서 발견한 핵심 발병 원인은 고포도당에 의해 혈관내피세포의 Jagged1 분자 발현이 증가한다는 것이다. 혈관내피세포들은 Notch 신호전달체계를 통해 서로 신호를 주고 받으며 안정상태를 유지하며 기능하는데, 본 연구에서는 당뇨병에 의해 증가된

Jagged1 분자에 의해 Notch 신호 전달 체계를 차단되고, 이로 인해 혈관내피세포의 세포간 결합을 약화되고 혈관이 위축 • 소멸되는 현상을 발견하였다.

더 나아가 증가된 Jagged1 을 인위적으로 감소시키면, 당뇨병으로 인해서 발생한 혈관합병증을 정상화시킬 수 있음을 당뇨병 쥐 모델에서 증명함으로써, 향후 당뇨 혈관병의 예방 및 신치료제 개발이 가능함을 보였다.

또한 본 연구 결과는 당뇨망막병, 당뇨콩팥병, 당뇨심근병, 당뇨발 및 말초혈관질환을 병태 생리를 이해하는 데에도 크게 기여할 것으로 보여 향후 당뇨혈관병 치료의 새로운 지평을 열 수 있을 것으로 기대한다.

주요어 : 당뇨, 당뇨 미세혈관병증의 기전, Notch 신호전달

학 번 : 2008-31033